# Estimating Water Fluxes Across the Sediment–Water Interface in the Lower Merced River, California



Scientific Investigations Report 2007–5216

# Estimating Water Fluxes Across the Sediment–Water Interface in the Lower Merced River, California

By Celia Zamora

For product and ordering information:
World Wide Web: http://www.usgs.gov/pubprod
Telephone: 1-888-ASK-USGS

For more information on the USGS--the Federal source for science about the Earth, its natural and living resources, natural hazards, and the environment:
World Wide Web: http://www.usgs.gov
Telephone: 1-888-ASK-USGS

# FOREWORD

The U.S. Geological Survey (USGS) is committed to providing the Nation with credible scientific information that helps to enhance and protect the overall quality of life and that facilitates effective management of water, biological, energy, and mineral resources (http://www.usgs.gov/). Information on the Nation's water resources is critical to ensuring long-term availability of water that is safe for drinking and recreation and is suitable for industry, irrigation, and fish and wildlife. Population growth and increasing demands for water make the availability of that water, now measured in terms of quantity and quality, even more essential to the long-term sustainability of our communities and ecosystems.

The USGS implemented the National Water-Quality Assessment (NAWQA) Program in 1991 to support national, regional, State, and local information needs and decisions related to water-quality management and policy (http://water.usgs.gov/nawqa). The NAWQA Program is designed to answer: What is the condition of our Nation's streams and ground water? How are conditions changing over time? How do natural features and human activities affect the quality of streams and ground water, and where are those effects most pronounced? By combining information on water chemistry, physical characteristics, stream habitat, and aquatic life, the NAWQA Program aims to provide science-based insights for current and emerging water issues and priorities. From 1991-2001, the NAWQA Program completed interdisciplinary assessments and established a baseline understanding of water-quality conditions in 51 of the Nation's river basins and aquifers, referred to as Study Units (http://water.usgs.gov/nawqa/studyu.html).

Multiple national and regional assessments are ongoing in the second decade (2001–2012) of the NAWQA Program as 42 of the 51 Study Units are reassessed. These assessments extend the findings in the Study Units by determining status and trends at sites that have been consistently monitored for more than a decade, and filling critical gaps in characterizing the quality of surface water and ground water. For example, increased emphasis has been placed on assessing the quality of source water and finished water associated with many of the Nation's largest community water systems. During the second decade, NAWQA is addressing five national priority topics that build an understanding of how natural features and human activities affect water quality, and establish links between *sources* of contaminants, the *transport* of those contaminants through the hydrologic system, and the potential *effects* of contaminants on humans and aquatic ecosystems. Included are topics on the fate of agricultural chemicals, effects of urbanization on stream ecosystems, bioaccumulation of mercury in stream ecosystems, effects of nutrient enrichment on aquatic ecosystems, and transport of contaminants to public-supply wells. These topical studies are conducted in those Study Units most affected by these issues; they comprise a set of multi-Study-Unit designs for systematic national assessment. In addition, national syntheses of information on pesticides, volatile organic compounds (VOCs), nutrients, selected trace elements, and aquatic ecology are continuing.

The USGS aims to disseminate credible, timely, and relevant science information to address practical and effective water-resource management and strategies that protect and restore water quality. We hope this NAWQA publication will provide you with insights and information to meet your needs, and will foster increased citizen awareness and involvement in the protection and restoration of our Nation's waters.

The USGS recognizes that a national assessment by a single program cannot address all water-resource issues of interest. External coordination at all levels is critical for cost-effective management, regulation, and conservation of our Nation's water resources. The NAWQA Program, therefore, depends on advice and information from other agencies—Federal, State, regional, interstate, Tribal, and local—as well as nongovernmental organizations, industry, academia, and other stakeholder groups. Your assistance and suggestions are greatly appreciated.

Robert M. Hirsch

Associate Director of Water

This page intentionally left blank.

# Contents

# Figures

# Tables

# Abbreviations and Acronyms

(Clarification or additional information given in parentheses)

| | |
|---|---|
| ACT | agricultural chemical transport |
| BW | bank well |
| i.d. | inside diameter |
| ID | identification |
| K | hydraulic conductivity |
| MW | monitoring well |
| NAWQA | National Water-Quality Assessment (USGS) |
| PVC | polyvinyl chloride |
| RPD | relative percent difference |
| RW | river well |
| VAMP | Vernalis Adaptive Management Plan |

### Organizations

| | |
|---|---|
| CDWR | California Department of Water Resources |
| MID | Modesto Irrigation District |
| USGS | U.S. Geological Survey |

### Units of measurement

| | |
|---|---|
| cm | centimeter |
| $cm^2$ | square centimeter |
| cm/day | centimeter per day |
| cm/s | centimeter per second |
| ft | foot (feet) |
| in. | inch |
| km | kilometer |
| $km^2$ | square kilometer |
| $km^3$ | cubic kilometer |
| m | meter |
| $m^2$ | square meter |
| $m^3$ | cubic meter |
| m/km | meter per kilometer |
| mi | mile |
| $m^3/s$ | cubic meter per second |
| mL | milliliter ($10^{-3}$ liter) |
| mL/min | milliliter per minute |
| mm | millimeter ($10^{-3}$ meter) |

**Notes:**

Temperature in degrees Celsius (°C) may be converted to degrees Fahrenheit (°F) as follows:

$$°F = (1.8 \times °C) + 32$$

Temperature in degrees Fahrenheit (°F) may be converted to degrees Celsius (°C) as follows:

$$°C = (°F - 32)/1.8$$

Vertical coordinate information is referenced to the North American Vertical Datum of 1988 (NAVD 88).

Horizontal coordinate information is referenced to the North American Datum of 1983 (NAD 83).

Altitude, as used in this report, refers to distance above the vertical datum.

This page intentionally left blank.

# Estimating Water Fluxes Across the Sediment–Water Interface in the Lower Merced River, California

By Celia Zamora

## Abstract

The lower Merced River Basin was chosen by the U.S. Geological Survey's (USGS) National Water Quality Assessment Program (NAWQA) to be included in a national study on how hydrological processes and agricultural practices interact to affect the transport and fate of agricultural chemicals. As part of this effort, surface-water–ground-water (sw–gw) interactions were studied in an instrumented 100-m reach on the lower Merced River. This study focused on estimating vertical rates of exchange across the sediment–water interface by direct measurement using seepage meters and by using temperature as a tracer coupled with numerical modeling. Temperature loggers and pressure transducers were placed in monitoring wells within the streambed and in the river to continuously monitor temperature and hydraulic head every 15 minutes from March 2004 to October 2005. One-dimensional modeling of heat and water flow was used to interpret the temperature and head observations and deduce the sw–gw fluxes using the USGS numerical model, VS2DH, which simulates variably saturated water flow and solves the energy transport equation. Results of the modeling effort indicate that the Merced River at the study reach is generally a slightly gaining stream with small head differences (cm) between the surface water and ground water, with flow reversals occurring during high streamflow events. The average vertical flux across the sediment–water interface was 0.4–2.2 cm/day, and the range of hydraulic conductivities was 1–10 m/day. Seepage meters generally failed to provide accurate data in this high-energy system because of slow seepage rates and a moving streambed resulting in scour or burial of the seepage meters. Estimates of streambed hydraulic conductivity were also made using grain-size analysis and slug tests. Estimated hydraulic conductivity for the upstream transect determined using slug tests ranged from 40 to 250 m/day, whereas the downstream transect ranged from 10 to 100 m/day. The range in variability was a result of position along each transect. A relative percent difference was used to describe the variability in estimates of hydraulic conductivity by grain-size analysis and slug test. Variability in applied methods at the upstream transect ranged from 0 to 9 percent, whereas the downstream transect showed greater variability, with a range of 80 to 133 percent.

## Introduction

Hydrologists traditionally regarded streams and ground water as distinct, independent resources to be utilized and managed separately. However, with increased demands on water supplies, hydrologists realized that streams and ground water are parts of a single, interconnected resource (Winter and others, 1998). Attempts to distinguish these resources for analytical or regulatory purposes often meet with difficulty because sustained depletions of one resource negatively impact the other. An understanding of the interconnections between surface water and ground water is therefore essential. Scientists have begun to show that local hydrologic interactions between surface water and ground water play an important role in stream ecosystem structure and function (Gilbert and others, 1994; Findlay, 1995; Brunke and Gonser, 1997). Water that passes back and forth between the surface water and subsurface water influences the fate and mobilization of trace metals and organic pollutants, and can enhance biogeochemical reactions that can affect downstream water quality. Understanding these interactions at small scales requires knowledge of ground-water flowpaths and their linkages to streams, rates of exchange between stream and ground-water systems, and the mechanisms that generate spatial (channel unit, reach, and watershed) and temporal (diel, seasonal) variations in these processes (Wroblicky and others, 1998). Rates of exchange across a streambed are most commonly estimated using one or more of the following approaches: (1) Darcy water-flux calculations, (2) tracer-based approaches, and (3) direct measurements across a streambed using a device such as a seepage meter. The Darcy approach calculates water fluxes across streambeds on the basis of two-dimensional maps of hydraulic head, estimates of hydraulic conductivity of near-channel sediment, and the basic governing equations for ground-water flow (Harvey and Wagner, 2000). The tracer approach lets one observe an introduced tracer (for example, salt, deionized water, or bromide) or an environmental tracer (temperature or specific conductance) to infer flux rates across the streambed. A seepage meter directly measures vertical flux across the sediment–water interface.

## Background

The Merced River, located in the San Joaquin River Basin in central California, was chosen by the U.S. Geological Survey's (USGS) National Water-Quality Assessment (NAWQA) Program as one of five study areas in a national study of how hydrological processes and agricultural practices interact to affect the transport and fate of agricultural chemicals in nationally important agricultural settings. The key to achieving this objective is an understanding of how the agricultural chemicals move through each hydrologic compartment, as well as estimating rates of exchange between compartments. Five hydrologic compartments were monitored: the atmosphere, surface water, the unsaturated zone, ground water, and the hyporheic zone (surface-water–ground-water, or sw–gw, interaction). This project focused on estimating rates of exchange between the surface water and ground water across the sediment–water interface in the lower Merced River, California.

Estimates of ground-water seepage were made along a 100-m reach in the lower Merced River. The site location was chosen on the basis of reconnaissance work. The criteria required that the reach be gaining, easily accessible, and located next to agricultural land on which agricultural chemicals of interest were being applied. The location of the reach also bracketed the end of the ground-water flowpath compartment and was near the atmosphere and unsaturated zone compartment in the adjacent almond orchard.

## Purpose and Scope

This report provides information regarding the use of seepage meters in a river environment and the application of temperature as a tracer in the shallow riverbed subsurface to predict rates of exchange using a USGS heat and flow model. Vertical estimates of ground-water seepage rates through a 100-m reach of the Merced River, California, are presented. Seepage rates were estimated directly using seepage meters, and indirectly using temperature and head measurements to calibrate a flow and heat transport model, VS2DH. Indirect seepage rates were constrained by hydraulic conductivity estimates from sieve analysis of streambed sediments and slug tests.

## Study Area

The study area is located in the lower Merced River Basin, which lies on the east side of the San Joaquin Valley in the San Joaquin Basin and is approximately 831 km$^2$ (fig.1). Two transects across a 100-m reach were equipped with monitoring wells that recorded continuous temperature and pressure head throughout the study period (fig. 2 and table 1). Table 1 describes the location and type of monitoring equipment depicted in figure 2. The lower Merced River Basin setting is predominately agriculture on the valley floor and lies within the flat structural basin of the San Joaquin Valley. The upstream part of the lower basin extends eastward into the lower foothills of the Sierra Nevada. The San Joaquin Valley is bounded by the Sierra Nevada to the east, the Coast Ranges to the west, the Tehachapi Mountains to the south, and the Sacramento–San Joaquin Delta to the north. The boundary of the basin is defined by the topographic drainage divides and in some areas, by canals and laterals that serve this area. The altitude ranges from 22 m in the San Joaquin Valley to 168 m above sea level in the Sierra Nevada foothills. Elevation gradients average about 2.5 m/km on the valley floor and 26.7 m/km in the foothills (Gronberg and Kratzer, 2006). Approximately 55 percent of the lower Merced River Basin is covered by agricultural land; 39 percent is forest, shrub land, and grassland; over 4 percent is urban and transitional land; and less than 2 percent is water and wetland (Vogelmann and others, 2001). The forest, shrub land, and grassland are predominantly on the valley floor.

## Geology

The San Joaquin Valley is part of the Central Valley, which is a large, northwest-trending, asymmetric structural trough, filled with marine and continental sediments (Bartow, 1991). To the east of the valley, the Sierra Nevada is composed primarily of pre-Tertiary granitic rocks and is separated from the valley by a foothill belt of marine and metavolcanic rocks. The Coast Ranges west of the valley are a complex assemblage of rocks, including marine and continental sediments of the Cretaceous to Quaternary Periods (Page, 1977; Page 1986). Alluvial deposits of the eastern part of the valley were derived primarily from the weathering of granitic instrusive rocks of the Sierra Nevada, and are highly permeable, medium- to coarse-grained sands with low total organic carbon, forming broad alluvial fans where the streams enter the valley. These deposits generally are coarsest near the upper parts of the alluvial fans and finest near the valley trough. Dune sand, derived from the alluvial deposits, consists of well-sorted medium-to-fine sand, as much as 43-m thick (Page, 1986). Stream-channel deposits along the Merced River consist of medium-to-coarse sand with silty-clay layers (~2 cm–60 cm) in the shallow subsurface.

Consolidated rocks and deposits exposed along the margin of the valley floor include Tertiary and Quaternary continental deposits, Cretaceous and Tertiary marine sedimentary rocks, and the pre-Tertiary Sierra Nevada basement complex (Davis and Hall, 1959; Croft, 1972; Page and Balding, 1973). Most of the unconsolidated deposits in the study area are contained within the Pliocene–Pleistocene Laguna, Turlock Lake, Riverbank, and Modesto Formations, with minor amounts of Holocene stream-channel and flood-basin deposits. The Turlock Lake, Riverbank, and Modesto Formations form a sequence of overlapping channel incisions that were influenced by climatic fluctuations, and resultant glacial stages in the Sierra Nevada (Bartow, 1991).
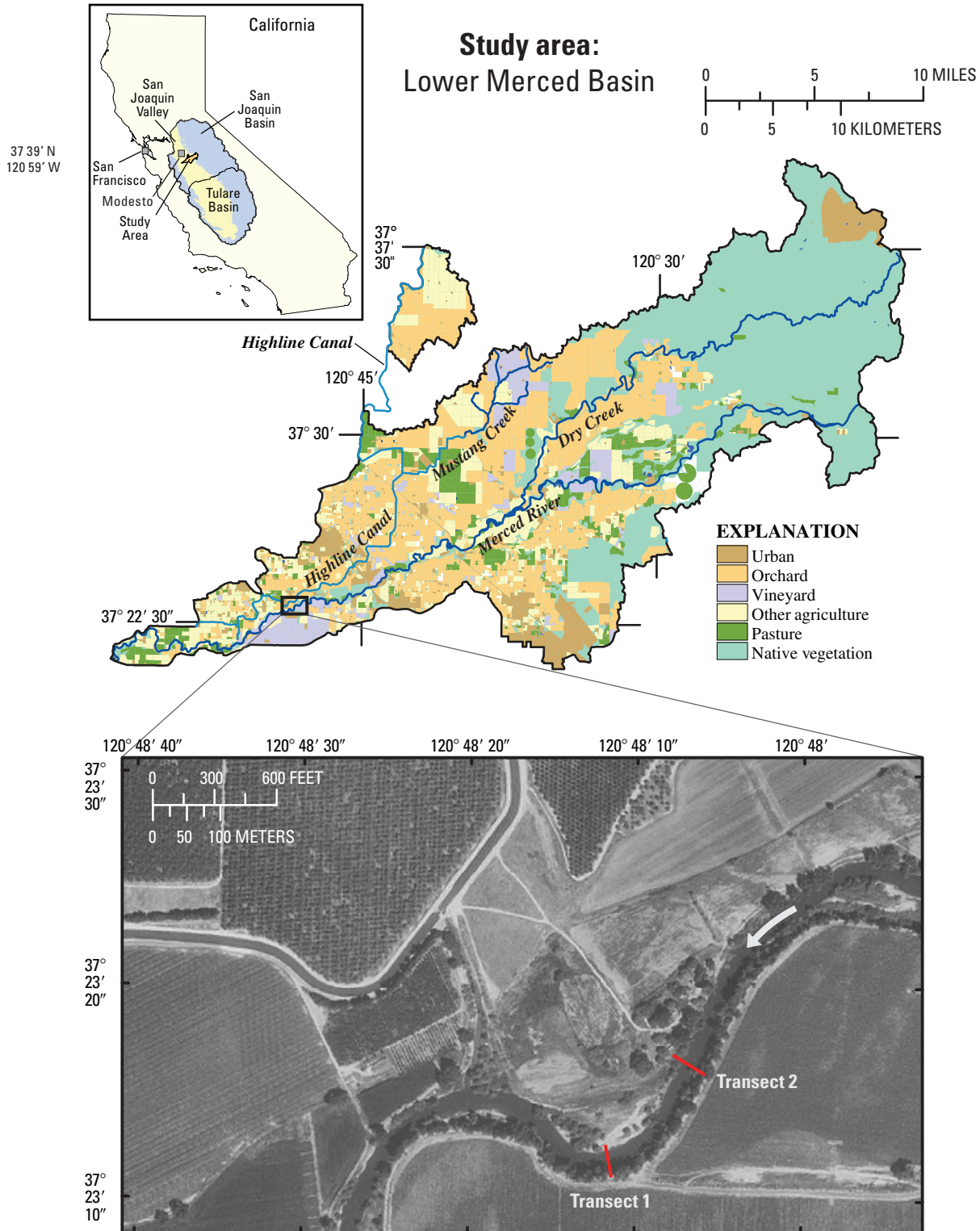
**Figure 1.** Study area and locations of fixed transect 1 and transect 2 in the lower Merced Basin. Arrow indicates direction of streamflow.
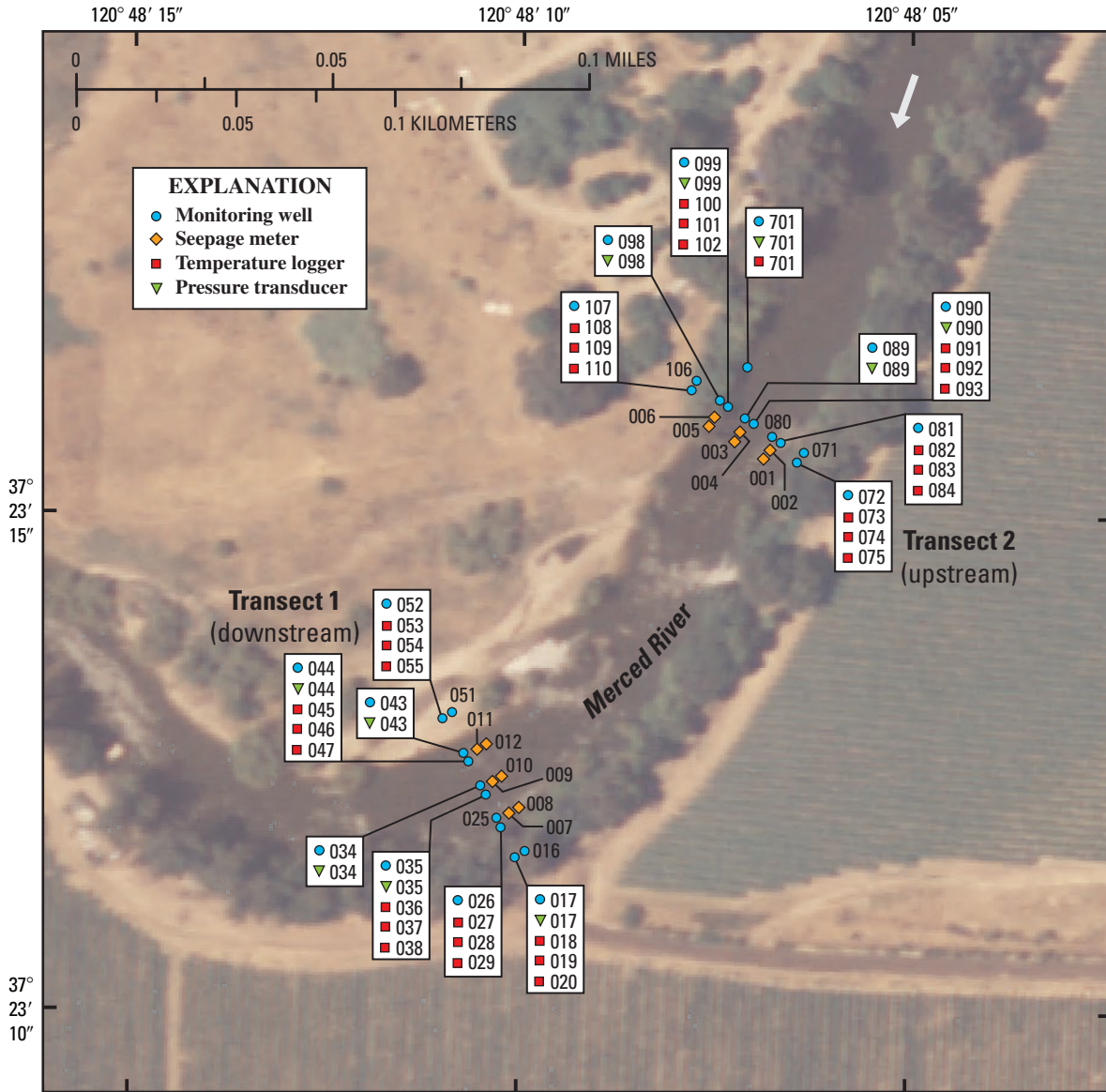
**Figure 2.** Location of monitoring wells and monitoring equipment at fixed transects 1 and 2 in the lower Merced Basin. Arrow in upper right on map indicates direction of streamflow.

The Corcoran Clay, at the base of the upper Turlock Lake Formation, is a lacustrine deposit that is a key subsurface feature in the San Joaquin Valley. Page (1986) mapped the areal extent of this regional aquitard on the basis of a limited number of well logs and geophysical logs. Additional lithologic data recently were used to modify the mapped extent of this important unit (Burow and others, 2004). The eastern extent of the Corcoran Clay roughly parallels the San Joaquin River valley axis. The Corcoran Clay ranges in depth from 28 to 85 m below land surface and a thickness from 0 to 57 m in the study area.

**Table 1.**   Description of monitoring equipment in monitoring wells used in this study that corresponds with depictions in figure 2.

[BLW, below; ID, identification; LSD, land surface datum;  M, m, meter; MI, mile; NR, near; PVC, polyvinyl chloride; R, river; TEMP, temperature; US, upstream; USGS, U.S. Geological Survey. Map symbols: ♦, seepage meter; ●, monitoring well; ▼, pressure transducer; ■ , temperature logger]

| Map ID number | Map symbol | Monitoring equipment | USGS site ID | USGS site name |
|---|---|---|---|---|
| 001 | ♦ | seepage meter | 372312120481001 | SEEPAGE METER "D" 11.2 MI US MERCED R NR STEVINSON |
| 002 | ♦ | seepage meter | 372312120481002 | SEEPAGE METER "4" 11.2 MI US MERCED R NR STEVINSON |
| 003 | ♦ | seepage meter | 372312120481003 | SEEPAGE METER "E" 11.2 MI US MERCED R NR STEVINSON |
| 004 | ♦ | seepage meter | 372312120481004 | SEEPAGE METER "5" 11.2 MI US MERCED R NR STEVINSON |
| 005 | ♦ | seepage meter | 372312120481005 | SEEPAGE METER "F" 11.2 MI US MERCED R NR STEVINSON |
| 006 | ♦ | seepage meter | 372312120481006 | SEEPAGE METER "6" 11.2 MI US MERCED R NR STEVINSON |
| 007 | ♦ | seepage meter | 372312120481007 | SEEPAGE METER "A" 11.3 MI US MERCED R NR STEVINSON |
| 008 | ♦ | seepage meter | 372312120481008 | SEEPAGE METER "1" 11.3 MI US MERCED R NR STEVINSON |
| 009 | ♦ | seepage meter | 372312120481009 | SEEPAGE METER "B" 11.3MI US MERCED R NR STEVINSON |
| 010 | ♦ | seepage meter | 372312120481010 | SEEAPGE METER "2" 11.3 MI US MERCED R NR STEVINSON |
| 011 | ♦ | seepage meter | 372312120481011 | SEEPAGE METER "C" 11.3 MI US MERCED R NR STEVINSON |
| 012 | ♦ | seepage meter | 372312120481012 | SEEPAGE METER "3" 11.3 MI US MERCED R NR STEVINSON |
| 016 | ● | monitoring well screened 3.5 m below land surface | 372312120481016 | 006S011E30B019M |
| 017 | ● | monitoring well screened 5 m below land surface | 372312120481017 | 006S011E30B018M |
| 017 | ▼ | pressure transducer | 372312120481017 | 006S011E30B018M |
| 018 | ■ | temperature logger 3.5 m below land surface | 372312120481018 | 006S011E30B018M WATER TEMP-LOGGER AT 350CM BLW PVC |
| 019 | ■ | temperature logger 4 m below land surface | 372312120481019 | 006S011E30B018M WATER TEMP-LOGGER AT 400CM BLW PVC |
| 020 | ■ | temperature logger 5 m below land surface | 372312120481020 | 006S011E30B018M WATER TEMP-LOGGER AT 500CM BLW PVC |
| 025 | ● | monitoring well screened 0.5 m below streambed | 372312120481025 | 006S011E30B017M |
| 026 | ● | monitoring well screened 3 m below streambed | 372312120481026 | 006S011E30B016M |
| 027 | ■ | temperature logger 0.5 m below streambed | 372312120481027 | 006S011E30B016M WATER TEMP LOGGER AT 0.5M BLW LSD |
| 028 | ■ | temperature logger 1 m below streambed | 372312120481028 | 006S011E30B016M WATER TEMP LOGGER AT 1.0M BLW LSD |
| 029 | ■ | temperature logger 2 m below streambed | 372312120481029 | 006S011E30B016M WATER TEMP LOGGER AT 2.0M BLW LSD |
| 034 | ● | monitoring well screened 0.5 m below streambed | 372312120481034 | 006S011E30B015M |
| 034 | ▼ | pressure transducer | 372312120481034 | 006S011E30B015M |
| 035 | ● | monitoring well screened 3 m below streambed | 372312120481035 | 006S011E30B014M |
| 035 | ▼ | pressure transducer | 372312120481035 | 006S011E30B014M |
| 036 | ■ | temperature logger 0.5 m below streambed | 372312120481036 | 006S011E30B014M WATER TEMP LOGGER AT 0.5M BLW LSD |

**Table 1.** Description of monitoring equipment in monitoring wells used in this study that corresponds with depictions in figure 2—Continued.

[BLW, below; ID, identification; LSD, land surface datum; M, m, meter; MI, mile; NR, near; PVC, polyvinyl chloride; R, river; TEMP, temperature; US, upstream; USGS, U.S. Geological Survey. Map symbols: ◆, seepage meter; ●, monitoring well; ▼, pressure transducer; ■, temperature logger]

| Map ID number | Map symbol | Monitoring equipment | USGS site ID | USGS site name |
|---|---|---|---|---|
| 037 | ■ | temperature logger 1.0 m below streambed | 372312120481037 | 006S011E30B014M WATER TEMP LOGGER AT 1.0M BLW LSD |
| 038 | ■ | temperature logger 2.0 m below streambed | 372312120481038 | 006S011E30B014M WATER TEMP LOGGER AT 2.0M BLW LSD |
| 043 | ● | monitoring well screened 0.5 m below streambed | 372312120481043 | 006S011E30B013M |
| 043 | ▼ | pressure transducer | 372312120481043 | 006S011E30B013M |
| 044 | ● | monitoring well screened 3 m below streambed | 372312120481044 | 006S011E30B012M |
| 044 | ▼ | pressure transducer | 372312120481044 | 006S011E30B012M |
| 045 | ■ | temperature logger 0.5 m below streambed | 372312120481045 | 006S011E30B012M WATER TEMP LOGGER AT 0.5M BLW LSD |
| 046 | ■ | temperature logger 1.0 m below streambed | 372312120481046 | 006S011E30B012M WATER TEMP LOGGER AT 1.0M BLW LSD |
| 047 | ■ | temperature logger 2.0 m below streambed | 372312120481047 | 006S011E30B012M WATER TEMP LOGGER AT 2.0M BLW LSD |
| 051 | ● | monitoring well screened 3.5 m below land surface | 372312120481051 | 006S011E30B011M |
| 052 | ● | monitoring well screened 5 m below land surface | 372312120481052 | 006S011E30B010M |
| 053 | ■ | temperature logger 3.5 m below land surface | 372312120481053 | 006S011E30B010M WATER TEMP-LOGGER AT 350CM BLW PVC |
| 054 | ■ | temperature logger 4 m below land surface | 372312120481054 | 006S011E30B010M WATER TEMP-LOGGER AT 400CM BLW PVC |
| 055 | ■ | temperature logger 5 m below land surface | 372312120481055 | 006S011E30B010M WATER TEMP-LOGGER AT 500CM BLW PVC |
| 071 | ● | monitoring well screened 3.5 m below land surface | 372312120481071 | 006S011E30B029M |
| 072 | ● | monitoring well screened 5 m below land surface | 372312120481072 | 006S011E30B028M |
| 073 | ■ | temperature logger 3.5 m below land surface | 372312120481073 | 006S011E30B028M WATER TEMP-LOGGER AT 350CM BLW PVC |
| 074 | ■ | temperature logger 4 m below land surface | 372312120481074 | 006S011E30B028M WATER TEMP-LOGGER AT 400CM BLW PVC |
| 075 | ■ | temperature logger 5 m below land surface | 372312120481075 | 006S011E30B028M WATER TEMP-LOGGER AT 500CM BLW PVC |
| 080 | ● | monitoring well screened 0.5 m below streambed | 372312120481080 | 006S011E30B027M |
| 081 | ● | monitoring well screened 3 m below streambed | 372312120481081 | 006S011E30B026M |
| 082 | ■ | temperature logger 0.5 m below streambed | 372312120481082 | 006S011E30B026M WATER TEMP LOGGER AT 0.5M BLW LSD |
| 083 | ■ | temperature logger 1 m below streambed | 372312120481083 | 006S011E30B026M WATER TEMP LOGGER AT 1.0M BLW LSD |
| 084 | ■ | temperature logger 2 m below streambed | 372312120481084 | 006S011E30B026M WATER TEMP LOGGER AT 2.0M BLW LSD |
| 089 | ● | monitoring well screened 0.5 m below streambed | 372312120481089 | 006S011E30B025M |
| 089 | ▼ | pressure transducer | 372312120481089 | 006S011E30B025M |
| 090 | ● | monitoring well screened 3 m below streambed | 372312120481090 | 006S011E30B024M |
| 090 | ▼ | pressure transducer | 372312120481090 | 006S011E30B024M |

**Table 1.** Description of monitoring equipment in monitoring wells used in this study that corresponds with depictions in figure 2—Continued.

[BLW, below; ID, identification; LSD, land surface datum;  M, m, meter; MI, mile; NR, near; PVC, polyvinyl chloride; R, river; TEMP, temperature; US, upstream; USGS, U.S. Geological Survey. Map symbols: ◆, seepage meter; ●, monitoring well; ▼, pressure transducer; ■, temperature logger]

| Map ID number | Map symbol | Monitoring equipment | USGS site ID | USGS site name |
|---|---|---|---|---|
| 091 | ■ | temperature logger 0.5 m below streambed | 372312120481091 | 006S011E30B024M WATER TEMP LOGGER AT 0.5M BLW LSD |
| 092 | ■ | temperature logger 1 m below streambed | 372312120481092 | 006S011E30B024M WATER TEMP LOGGER AT 1.0M BLW LSD |
| 093 | ■ | temperature logger 2 m below streambed | 372312120481093 | 006S011E30B024M WATER TEMP LOGGER AT 2.0M BLW LSD |
| 098 | ● | monitoring well screened 0.5 m below streambed | 372312120481098 | 006S011E30B023M |
| 098 | ▼ | pressure transducer | 372312120481098 | 006S011E30B023M |
| 099 | ● | monitoring well screened 3 m below streambed | 372312120481099 | 006S011E30B022M |
| 099 | ▼ | pressure transducer | 372312120481099 | 006S011E30B022M |
| 100 | ■ | temperature logger 0.5 m below streambed | 372312120481100 | 006S011E30B022M WATER TEMP LOGGER AT 0.5M BLW LSD |
| 101 | ■ | temperature logger 1 m below streambed | 372312120481101 | 006S011E30B022M WATER TEMP LOGGER AT 1.0M BLW LSD |
| 102 | ■ | temperature logger 2 m below streambed | 372312120481102 | 006S011E30B022M WATER TEMP LOGGER AT 2.0M BLW LSD |
| 106 | ● | monitoring well screened 3.5 m below land surface | 372312120481106 | 006S011E30B021M |
| 107 | ● | monitoring well screened 5 m below land surface | 372312120481107 | 006S011E30B020M |
| 108 | ■ | temperature logger 3.5 m below land surface | 372312120481108 | 006S011E30B020M WATER TEMP-LOGGER AT 350CM BLW PVC |
| 109 | ■ | temperature logger 4 m below land surface | 372312120481109 | 006S011E30B020M WATER TEMP-LOGGER AT 400CM BLW PVC |
| 110 | ■ | temperature logger 5 m below land surface | 372312120481110 | 006S011E30B020M WATER TEMP-LOGGER AT 500CM BLW PVC |
| 701 | ● | monitoring well screened above sediment/water interface | 372316120480701 | MERCED R NR RIVER MILE 16 NR DELHI CA |
| 701 | ▼ | pressure transducer | 372316120480701 | MERCED R NR RIVER MILE 16 NR DELHI CA |
| 701 | ■ | temperature logger | 372316120480701 | MERCED R NR RIVER MILE 16 NR DELHI CA |

## Climate

The San Joaquin Valley has an arid-to-semiarid climate that is characterized by hot summers and mild winters. Average temperatures are fairly uniform over the valley floor. Temperature decreases with increasing elevation in the foothills and mountains of the Sierra Nevada. Long-term records for temperature do not exist for sites within the lower Merced River Basin. However, the Modesto Irrigation District (MID) has temperature data for downtown Modesto from 1939 to 2005 (Modesto Irrigation District, 2005). Mean low temperatures in degrees Fahrenheit range from mid-30s in the winter months to upper 50s in the summer. Mean high temperatures in degrees Fahrenheit range from mid-50s in the winter months to mid-90s in the summer (Gronberg and Kratzer, 2006). As with temperature, long-term precipitation records do not exist within the lower Merced River Basin. However, MID does have long-term precipitation record for Modesto from 1889 to 2005. Mean annual precipitation (1889–2005) in Modesto is 31 cm, but annual precipitation is highly variable. Eighty percent of the precipitation falls during November through March, with the maximum precipitation in December through February.

## Surface-Water Hydrology

The surface-water hydrology of the Merced River Basin has been significantly modified by the development of water resources. Between the 1870s and early 1900s, many canals were constructed to transport water to the land. Exchequer Dam was completed in 1926 to provide flood control and water for irrigation and power generation. In 1967, New Exchequer Dam was completed to expand Lake McClure Reservoir's capacity to 1.26 km$^3$. In the same year, McSwain Dam was completed downstream as a regulating reservoir. Downstream of McSwain Dam, the Merced Falls Dam diverts flow into the MID's Northside Canal to provide irrigation water to areas north of the Merced River. Farther downstream, Crocker-Huffman Dam diverts flow into the MID's Main Canal (Stillwater Sciences and EDAW, 2001). The area of focus for this study, the lower Merced River Basin, starts at New Exchequer Dam. Water quality above this point generally is unaffected by agricultural activities. The lower Merced River receives water from Dry Creek and from Mustang Creek by way of the Highline Canal.

Mean annual streamflow measured at the California Department of Water Resources (CDWR) Merced River near Stevinson gaging station (24 km downstream of the study site) is approximately 19.6 m$^3$/s for water years 1941–2005. Mean annual streamflow for this period varies greatly from year to year. The recent water years 2003–2004 had below-normal streamflow, whereas 2005 had above-average streamflow attributed to above-average snow pack in the Sierra Nevada above New Exchequer Dam (fig. 3). In a natural basin, the usual trend is to see a higher streamflow downstream as the area of contribution increases. However, because the Merced River is highly engineered and utilized for agricultural irrigation, it has an overall decrease in streamflow from the upper basin to the mouth.

## Ground-Water Hydrology

Ground water in the lower Merced Basin occurs primarily in the unconfined aquifer above and east of the Corcoran Clay and in the confined aquifer beneath the Corcoran Clay. The unconfined aquifer above the clay ranges in thickness from about 40 to 70 m. The unconfined aquifers east of the clay are composed primarily of alluvial sediment, but include the upper part of the Mehrten Formation, which is more consolidated than the overlying formations. The confined aquifer is composed of alluvial sediments and upper Mehrten Formation sediments from beneath the clay to the base of fresh water (Steven Phillips, USGS, written commun., 2006).
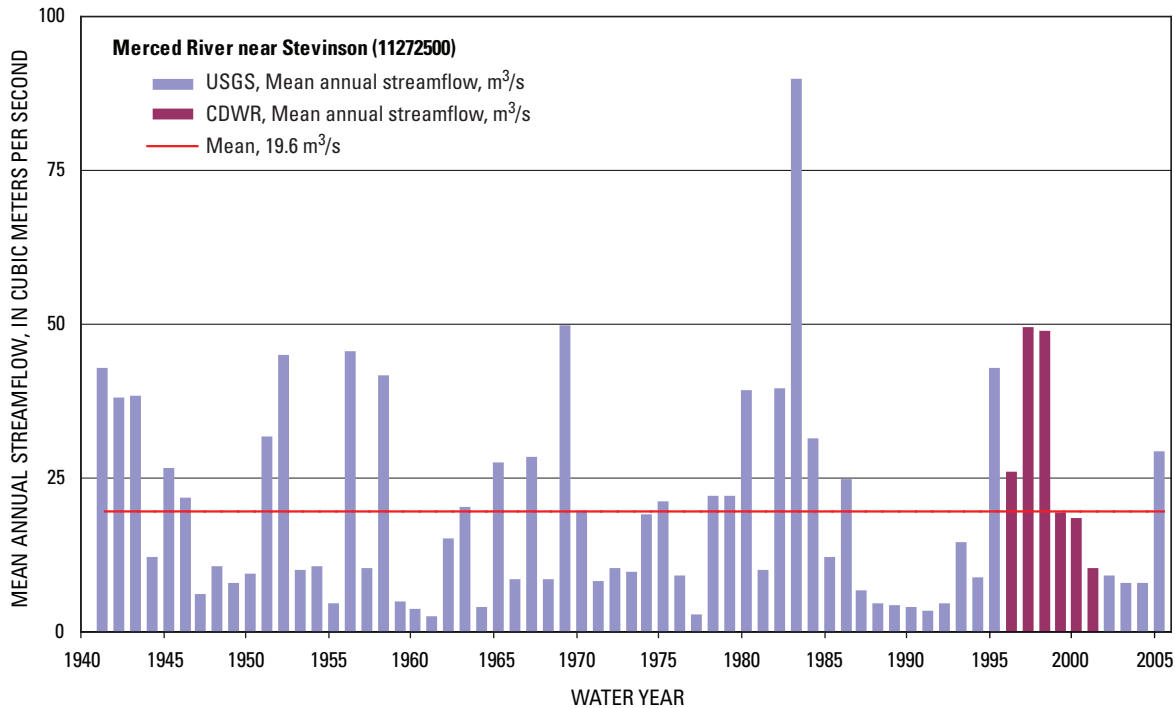


**Figure 3.**    Mean annual streamflow, Merced River near Stevinson, California, water years 1941–2005 (from California Department of Water Resources, 2006). Number in parentheses is the USGS site identification number (CDWR, California Department of Water Resources; m$^3$/s, cubic meters per second; USGS, U.S. Geological Survey).

Under natural conditions, ground-water recharge occurs primarily at the upper parts of the alluvial fans from streams entering the valley. Prior to ground-water resource development, most ground water had been discharged as evapotranspiration in the central trough of the valley, and to a lesser extent, to streams. Water-resource development in the basin has changed the ground-water flow regime. Pumping for agricultural irrigation and irrigation return flows are much greater than natural recharge and discharge and cause an increase in vertical flow in the system. Ground-water flow is generally toward the southwest and is somewhat similar to the predevelopment flow regime (Gronberg and Kratzer, 2006). However, ground water moving along a horizontal flowpath commonly is extracted by wells and reapplied at the surface several times before reaching the valley trough (Steven Phillips, USGS, written commun., 2006).

# Seepage Measurements

The seepage meter allows direct measurement of seepage flux across the sediment–water interface. It consists of a bottomless cylinder formed from an inverted drum or bucket connected to a collection bag by a length of tubing. The device is pushed into the bed of a lake or stream, and a collection bag with a known volume of water is attached. The collection bag is then removed after a period of elapsed time, and the rate of vertical ground-water flux through the area enclosed by the seepage meter is calculated from the increase or decrease in the initial volume of water, the length of time elapsed, and the area of the seepage meter, yielding flux rates in units of length/time. An increase in the initial volume indicates a positive vertical flux rate (ground water to surface water), and a decrease in initial volume indicates a negative vertical flux rate (surface water to ground water).

## Review of Literature

The seepage meter was initially developed to measure losses from irrigation canals (Israelsen and Reeve, 1944), and in the mid-1970s, the design was improved and the use was expanded to measure ground-water discharge into lakes (Lee, 1977; Lee and Cherry, 1978; John and Lock, 1977; Connor and Belanger, 1981; Erickson, 1981; Woessner and Sullivan, 1984; Isiorho and Matisoff, 1990; Shaw and Prepas, 1990b; Lesack, 1995; Rosenberry, 2000; Sebestyen and Schneider, 2001). Because seepage meters provide a quick and simple method for gathering information on the direction, rate, and variability of seepage flux across the sediment–water interface, their use has been expanded to environments other than lakes. Vertical seepage rates have been measured in wetlands (Choi and Harvey, 2000), estuaries (Lee, 1977; Lock and John, 1978; Zimmerman and others, 1985; Yelverton and Hackney, 1986; Boyle, 1994; Linderfelt and Turner, 2001) and nearshore ocean margins (Cable and others, 1997; Shinn and others, 2002;

Taniguchi, 2002; Chanton and others, 2003). Seepage meters have also been used to determine water budgets (Fellows and Brezonik, 1980) or to obtain samples for chemical analysis (Lee, 1977; Downing and Perterka, 1978; Brock and others, 1982; Belanger and Mikutel, 1985; Shaw and others, 1990).

A growing interest in investigating the rates of exchange between streams and ground water has led to the use of seepage meters in stream channels (Lee and Hynes, 1977; Connor and Belanger, 1981; McBride, 1987; Libelo and MacIntyre, 1994; Blanchefield and Ridgeway, 1996; Jackman and others, 1997; Cey and others, 1998; Fryar and others 2000; Dumouchelle, 2001; Landon and others, 2001; Murdoch and Kelly, 2003). However, the data obtained are often highly variable because the original design and application were intended for lake and estuary environments, where issues of current and scour are generally negligible. As discussed in more detail later in this section, significant streamflow rates may create hydraulic pressure on the measure bag, creating erroneous gains or losses in the bag volume over time. Scour may lead to a breach in the hydraulic seal around the seepage meter. Flume and laboratory studies show that much of this variation is due to the effects of flow across the seepage meter collection bag, which alters the hydraulic head within the meter and induces seepage flow (Libelo and MacIntyre, 1994). Their study discovered that the induced seepage flow can be significantly reduced by isolating the seepage meter collection bag from the streamflow.

Concerns over the effects that size, thickness, and initial conditions of the attached collection bag have on measured seepage rates have prompted investigations in field and laboratory settings. Shaw and Prepas (1989) found that an anomalous, short-term influx of water into seepage meters occurred immediately after connecting the collection bag to the seepage meter, but showed that the anomaly could be effectively eliminated by attaching prefilled collection bags with a minimum of 1,000 mL before attaching to the seepage meter. The effects of bag type and meter size on seepage-meter measurements were evaluated in a laboratory setting by Isiorho and Meyer (1999). Their study found that there was no significant difference attributed to bag type, but found that smaller diameter seepage meters had a greater variance. Laboratory studies have also examined bag conductance, which is the ratio of the volumetric flow rate into the bag to the hydraulic head required to fill the bag (Murdoch and Kelly, 2003). Harvey and Lee (2000) found that the conductance of a bag formed from a thin compliant film is expected to be large and relatively constant until it is filled with enough water to cause stretching, at which point conductance will decrease. The conductance of a bag may also vary if the bag deforms in an irregular manner and will decrease if kinks or folds develop in the bag (Kelly, 2001). As a collection bag opens and approaches its manufactured shape, a gradual decrease in conductance of the bag with increasing volume was observed by Schincariol and McNeil (2002). Similar results were observed by Shaw and Prepas (1989) and Blanchfield and Ridgeway (1996).

In field settings, slow seepage rates and the relatively small area measured also present problems. Very slow seepage rates may require a meter to be in place for several days. The problem of measurement area is of concern because most researchers and watershed managers are interested in seepage processes on a scale of hundreds to thousands of square meters or more, and most seepage meters typically integrate vertical flux over an area of approximately 0.25 m$^2$ or less (Rosenberry, 2005). Rosenberry addressed these issues in a low-permeability zone by connecting multiple seepage meter cylinders together to a single collection bag to increase the area represented by each measurement, thus integrating spatial heterogeneity over a larger area and reducing the time required to collect a measurable change in volume.

Some investigators (Erickson, 1981; Brock and others, 1982; Woessner and Sullivan, 1984; Shaw and Prepas, 1990a; Blanchfield and Ridgeway, 1996; Harvey and Lee, 2000) using seepage meters have expressed guarded concerns that the performance of the meter itself may cause variability that is unrelated to, and can obscure, the natural processes that they are trying to characterize (Schincariol and McNeil, 2002). Erickson (1981) stated that seepage meters disturb the flow field in which they are installed, resulting in consistently lower measured seepage rates. This disturbance is apparently related to frictional resistance along the internal boundaries of the meter. Frictional resistance is inherent to some extent in all seepage meter designs, and as a result, several laboratory studies have come up with a seepage meter coefficient that is used to convert measured seepage rates to true values. Coefficients in the literature range from 1.1 to 1.7 (Erickson, 1981; Cherkauer and McBride, 1988; Asbury, 1990; Belanger and Montgomery, 1992). Many of the less efficient meter designs require larger coefficients primarily because they use small-diameter tubing to connect the bag to the seepage cylinder (Rosenberry, 2005). The use of large-diameter plumbing greatly reduces loss of efficiency, resulting in a smaller correction coefficient (Fellows and Brezonik, 1980; Rosenberry, 2005).

Murdoch and Kelly (2003) developed a theoretical analysis to evaluate the extent to which bag conductance and velocity head may affect flux measurements by a seepage meter. Their analysis showed that bag conductance, radius of the seepage meter, and hydraulic conductivity of the streambed can be combined to give a dimensionless term that characterizes seepage meter performance. Some seepage meters use electronic flowmeters (Paulsen and others, 2001; Taniguchi and Fukuo, 1993; Rosenberry and Morin, 2004) to eliminate problems encountered with the collection bag. Although these devices show promise, their availability and expense make their use limited. This study focused on the conventional seepage meter that is both inexpensive and easily fabricated.

The purpose of using seepage meters to directly measure seepage rates was to gain an overall understanding of the direction, rate, and variability of seepage rates within the study area. The seepage meters used in this study incorporated suggestions made by several investigators (Libelo and MacIntyre, 1994; Shaw and Prepas, 1989; Kelly, 2001; Murdoch and Kelly, 2003) in an attempt to minimize variability in measured vertical seepage rates. The performance of the collection bags used in this study was measured in a laboratory test tank, and improvements were made to seepage meters and collection bags as a result of laboratory test results.

## Field Measurements

### Field Methods

Flux rates across the sediment–water interface were measured directly using twelve drum-style (Lee, 1977) seepage meters. Two sizes of seepage meters were used: the larger meters were 2,500 cm$^2$ in cross-sectional area and 26.5-cm deep, and the smaller meters were 620 cm$^2$ in cross-sectional area and 13.5-cm deep. The field deployment methods for both sizes of meters was to carefully push each meter into the riverbed sediment, leaving approximately 5 cm of the top of each meter above the streambed bottom. The deployment array of the seepage meters placed in the streambed involved pairing a large and small seepage meter spaced approximately 1.5 m apart. The purpose of pairing the meters was to compare flux rates between seepage meter pairs and observe variability in measured rates for the same size meter at different parts of the array over consecutive measurements. Two deployment arrays were used throughout the study. The first deployment array involved placing the six paired meters perpendicular to flow across two transects that were separated by a distance of approximately 10 m, and the second deployment array placed the paired meters across two transects separated by a distance of approximately 100 m (fig. 4). The seepage-meter pairs will be referred to as A-1, B-2, C-3, and so on.

The meters were then left undisturbed for 12 to 24 hours to allow trapped air to escape, as well as to permit riverbed sediments to return to equilibrium after being disturbed during installation. Once deployed, the meters were left in place for the duration of the measuring event. Following the equilibration period, the collection bags were prefilled with 500–1,000 mL of water, placed in housing units to protect the bag from the flow of the river, and connected to the seepage meters. The collection bags and housing units were connected to the seepage meters using a 61-cm length of 0.64-cm-i.d. (inside diameter) vinyl tubing. The housing unit for the large, seepage-meter bag was a perforated plastic storage box that was secured to the top of the seepage meter with a bungee cord. The small seepage meter used the half of a drum as the housing unit for the collection bag and was simply pushed into the sediment alongside the seepage meter (figs. 5 and 6).
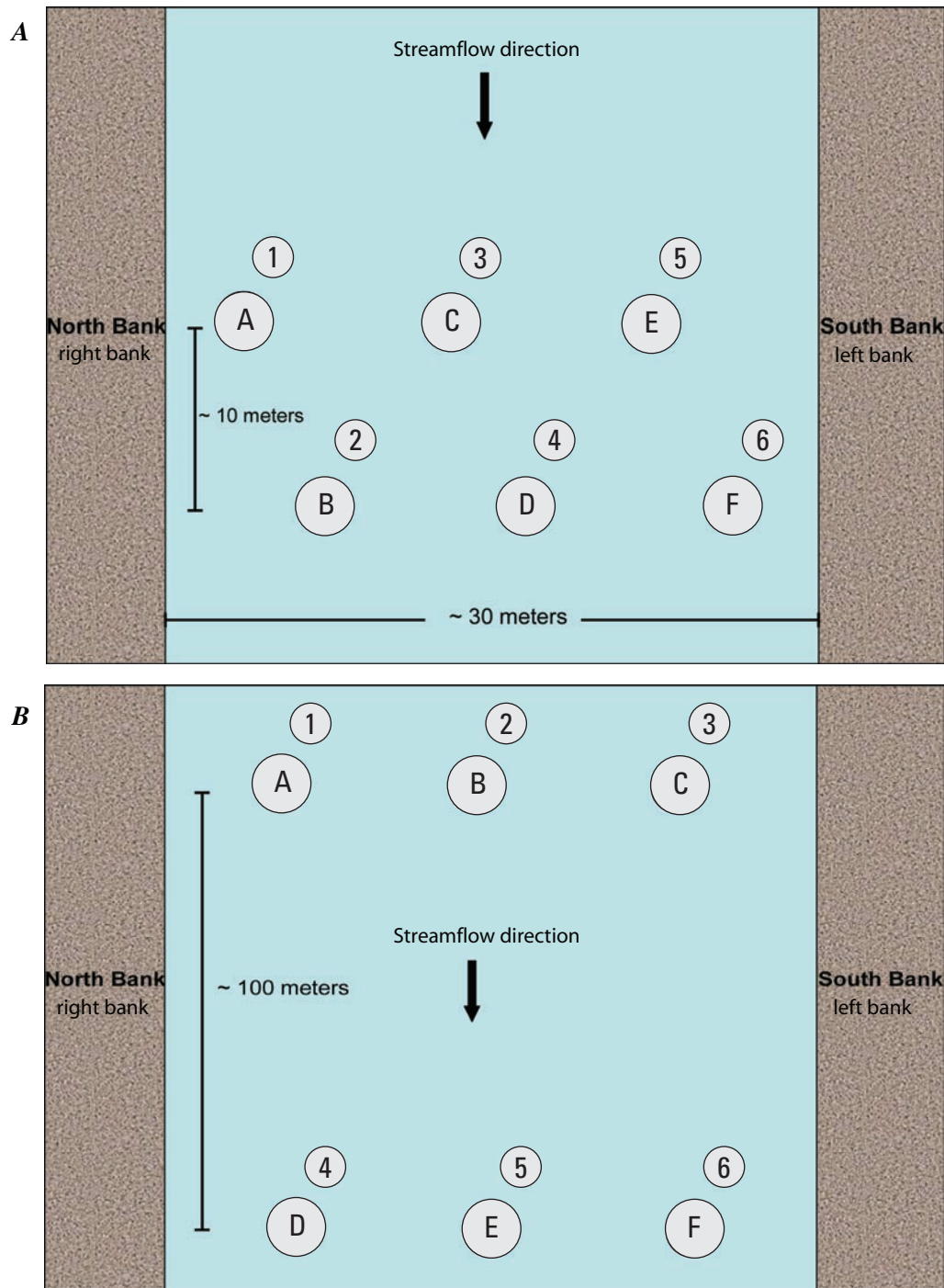
**Figure 4.**    Seepage meter arrays at transects 1 and 2. A. Array 1. B. Array 2.

Careful attention was given to avoid disturbing the sediments around each of the paired meters, and the attachment and retrieval of collection bags was performed by snorkeling to and from each meter to eliminate any contact with the riverbed bottom. Because of the slow flux rates encountered, the collection bags were retrieved and redeployed approximately every 12–24 hours over a few days. The change in volume was either measured using a graduated cylinder or weighed with a scale, and the elapsed time was recorded. The change in volume (mL/min) over the elapsed time (days) was divided by the cross-sectional area of the seepage meter ($cm^2$) to obtain vertical flux rates in cm/day.

*A*

*B*



**Figure 5.**    Seepage meters. A. Large seepage meter with attached housing unit. B. Small seepage meter with housing unit.



Streamflow direction

**Figure 6.**    Field deployment of paired seepage meters.

Three types of collection bags were used in the study. The collection bag types used were an 1,800-mL Sun Shower Solar Bag, a 2,000-mL medical urine collection bag, and a 2,000-mL Void-Fill packaging bag. These collection bags will be referred to as shower bag, medical bag, and packaging bag, respectively. Initial field measurements used only the shower and medical collection bags attached to the large and small seepage meters, respectively. However, the results of laboratory test runs prompted exclusive use of the packaging collection bag in seepage rate measurements made in the latter part of the study.

A total of six sampling events were made over a period of 10 months beginning in December 2003 and ending in September 2004. The planned period for each field measurement was initially intended to be one week. However, stream scour around the seepage meters resulted in only two or three repeat measurements taken over 48–72 hours. Because improvements were made to the seepage meter and collection bags over the period of the study, the objective and methods of each field visit are discussed individually and are listed in table 2.

## Field Results

Seepage meters did not work because of bed load movement in the upper 0.5 m of the Merced River. Observations of the streambed during site visits revealed that the stream bottom is continually moving—small dunes would develop and disappear several hours later. The problem was further compounded by the slow seepage rates, which required the seepage meters to be in place for several days and be subjected to the moving streambed, resulting in scour at the base of the meter(s) (fig. 7). Scoured-out seepage meters took in river water and filled the collection bag to maximum capacity, resulting in erroneously high seepage rates. In addition, the housing unit for the small seepage meter was not as effective as the housing unit for the large seepage meter. The housing units would scour out, become dislodged, and expose the collection bag to the flow of the river, thereby inducing volumetric flow into the collection bag. In other cases, the housing unit would become buried under the streambed sediments resulting in complete loss of initial volume.

The original intent of pairing the seepage meters was to compare flux rates between the two sizes. In most cases, the flux direction was opposing, and for pairs in which the flux direction was the same for both sizes, the difference in rates often was too great to provide meaningful results. In addition, variability existed in the measured flux rates between the same size meters over consecutive measurement periods. Low flux rates (<3 cm/day) and a moving streambed resulted in scour or burial of seepage meters. As a result, only two consecutive 24-hour measurement periods could be made for each seepage meter. Figures 8, 9, and 10 depict the variability in measurements described above for each meter over the six

sampling events. The Appendix lists the results of each of the six sampling events.

The smaller seepage meters (numbered seepage meters in figs. 8, 9, and 10) showed greater variability over consecutive measurements than the larger seepage meters, consistent with the findings of Isiorho and Meyer (1999). The results of the January and February 2004 (sampling events 3 and 4) gave inconclusive results for comparisons made between measured rates using shower and medical collection bags and comparison of those rates with measured rates using the packaging bags (Appendix). However, repeat measurements made with the shower bag attached to the large seepage meter gave consistent results. During the January 2004 visit, seepage meter B measured rates of 0.21 and 0.24 cm/day in two repeat measurements, and seepage meter C measured the same seepage rate, 0.15 cm/day, over a 48-hour period. The same pattern resulted for seepage meter A during the February 2004 visit, which measured a flux rate of 0.20 and 0.17 cm/day for consecutive measurements. The July and September 2004 site visits (sampling events 5 and 6) used only the thin-walled packaging bags attached to both meters, and inconsistencies in direction and magnitude of measured rates indicated no apparent pattern in seepage rates.

It was unclear whether the variability observed between the two types of seepage meters was a result of spatial variability in the hyporheic flowpaths at the sediment–water interface, a result of scour and burial problems encountered with the seepage meters, or unexplainable factors affecting the performance of the seepage meters and (or) collection bags. Because only two or three repeat measurements could be made at each of the field visits before the meters were scoured out, the seepage rates of pairs giving similar estimates are difficult to accept. More repeat measurements should be conducted before accepting the estimates of flux using this method. In addition, measurements should be made every 4–6 hours for several days to examine the response of seepage rates to diurnal variations in stream temperature and discharge resulting from evapotranspiration.

Evapotranspiration losses attributed to stream evaporation, stream-bank evaporation, and transpiration from stream channel vegetation create diurnal discharge patterns that are characterized by decreasing stream discharge during the day, with minimum discharge generally occurring in the afternoon (Taylor and Nickle, 1936; Troxell, 1936a,b). The decrease in discharge results in increased temperature variations downstream. The traditional assumption that reduced afternoon discharge is due entirely to evapotranspiration losses (Penman, 1963; Wisler and Brater, 1959) does not consider the importance of diurnal variations in stream temperature influencing seepage losses. A study conducted by Constantz and others (1994) demonstrates that for losing reaches with significant diurnal variations in stream temperature, the effect of stream temperature on streambed seepage is a major factor contributing to reduced streamflows. Studies using applied methods should incorporate quantitative analysis of diurnal stream–ground water interaction.

**Table 2.**   Objective and description of field measurements using seepage meters.

[Bag manufacturers: shower bag—Sun Solar Shower bag; medical bag—Medical Supply Bag; packaging bag—Void Packaging, Inc.]

| Sampling event | Field measurement period | Seepage meter array | Seepage meter size | Bag type | Objective |
|---|---|---|---|---|---|
| 1 | December 1–4, 2003 | 1 | large | shower bag | Compare seepage rates between bag types and paired meters. |
| | | | small | medical bag | |
| 2 | January 28–29, 2004 | 1 | large | shower bag | Compare measured rates using shower and medical bags in first 24-hour period to measured rates using only packaging bags in second 24-hr period. |
| | | | small | medical bag | |
| | January 29–30, 2004 | 1 | large | packaging bag | |
| | | | small | packaging bag | |
| 3 | February 10–11, 2004 | 1 | large | shower bag | Compare measured rates using shower and medical bags in first 24-hour period to measured rates using only packaging bags in second 24-hr period. |
| | | | small | medical bag | |
| | February 11–12, 2004 | 1 | large | packaging bag | |
| | | | small | packaging bag | |
| 4 | July 20–21, 2004 | 2 | large | packaging bag | Compare measured rates between repeat measurements using same bag types and compare measured rates between seepage meters. |
| | | | small | packaging bag | |
| | July 21–22, 2004 | 2 | large | packaging bag | |
| | | | small | packaging bag | |
| 5 | September 21–22, 2004 | 2 | large | packaging bag | Compare measured rates between repeat measurements using same bag types and compare measured rates between seepage meters. |
| | | | small | packaging bag | |
| | September 22–23, 2004 | 2 | large | packaging bag | |
| | | | small | packaging bag | |
| 6 | September 22–23, 2004 | 2 | large | packaging bag | Compare measured rates between repeat measurements using same bag types and compare measured rates between seepage meters. |
| | | | small | packaging bag | |
| | September 23–24, 2004 | 2 | large | packaging bag | |
| | | | small | packaging bag | |

Overall, the direct measurement technique as applied to this study resulted in inconclusive flux results. The moving streambed bottom seemed to be the limiting factor in applying this simple technique and overcame any other attempts to limit variability caused by the measurement technique. The seepage meters seemed to fail in this relatively high energy stream with its mobile bed.

## Laboratory Measurements

### Laboratory Methods

The performance of the three types of collection bags used in this study was tested in a laboratory seepage tank to examine the effects of bag thickness on measured rates of vertical flux. A cylindrical test tank with an inside diameter and height of 152 cm contained a 91-cm thick layer (1.67 m$^3$) of medium sand placed over a 15-cm layer (0.28 m$^3$) well-sorted, rounded gravel, with a medium size of 1.9 cm ([fig. 11](#)). Vertical flux was generated within the tank by introducing a constant headwater source to the bottom of the tank, and flow was measured by an in-line flow meter. A data logger recorded both the flow rate delivered to the bottom of the tank and pressure head measured by a pressure transducer located in the constant head water source tank. The data logger was programmed to control the pump to maintain a constant water level. An overflow opening was used to maintain water level within the constant head source tank to within 0.15 cm inside the tank.
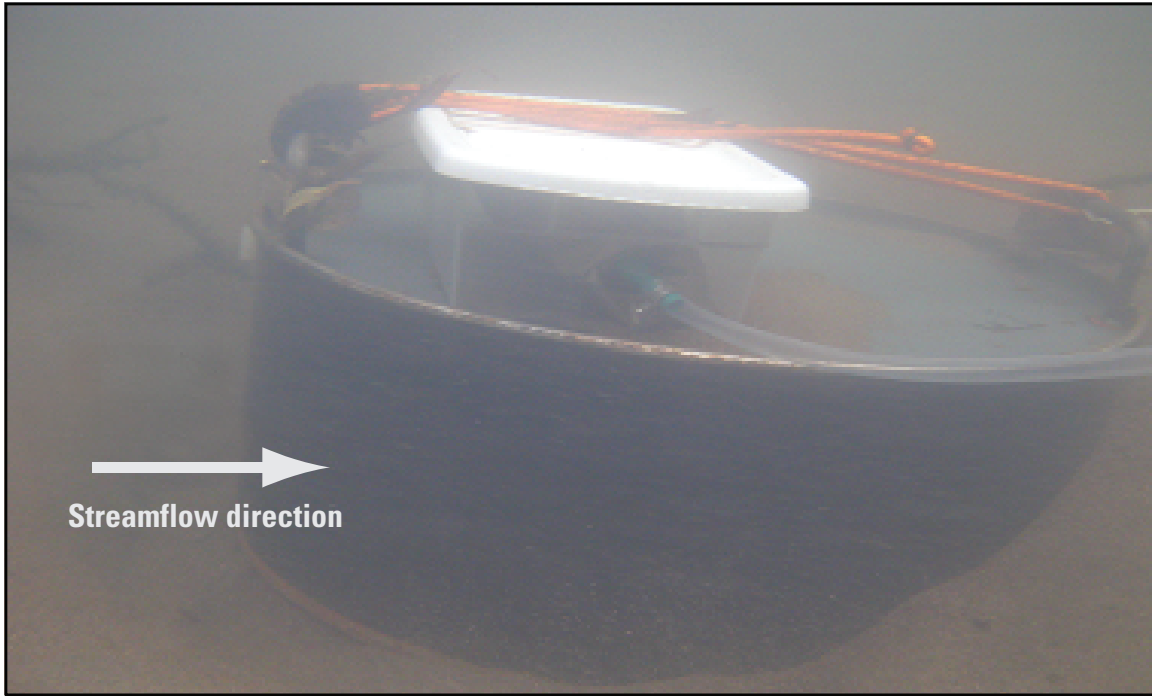
**Figure 7.** Scouring of streambed around seepage meter typically encountered 48 hours after deployment.



**Figure 8.** Measured vertical flux rates over consecutive 24-hour measurement periods for seepage meter pairs A-1 and B-2. A. Seepage meter A. B. Seepage meter B. C. Seepage meter 1. D. Seepage meter 2. (hr, hour.)
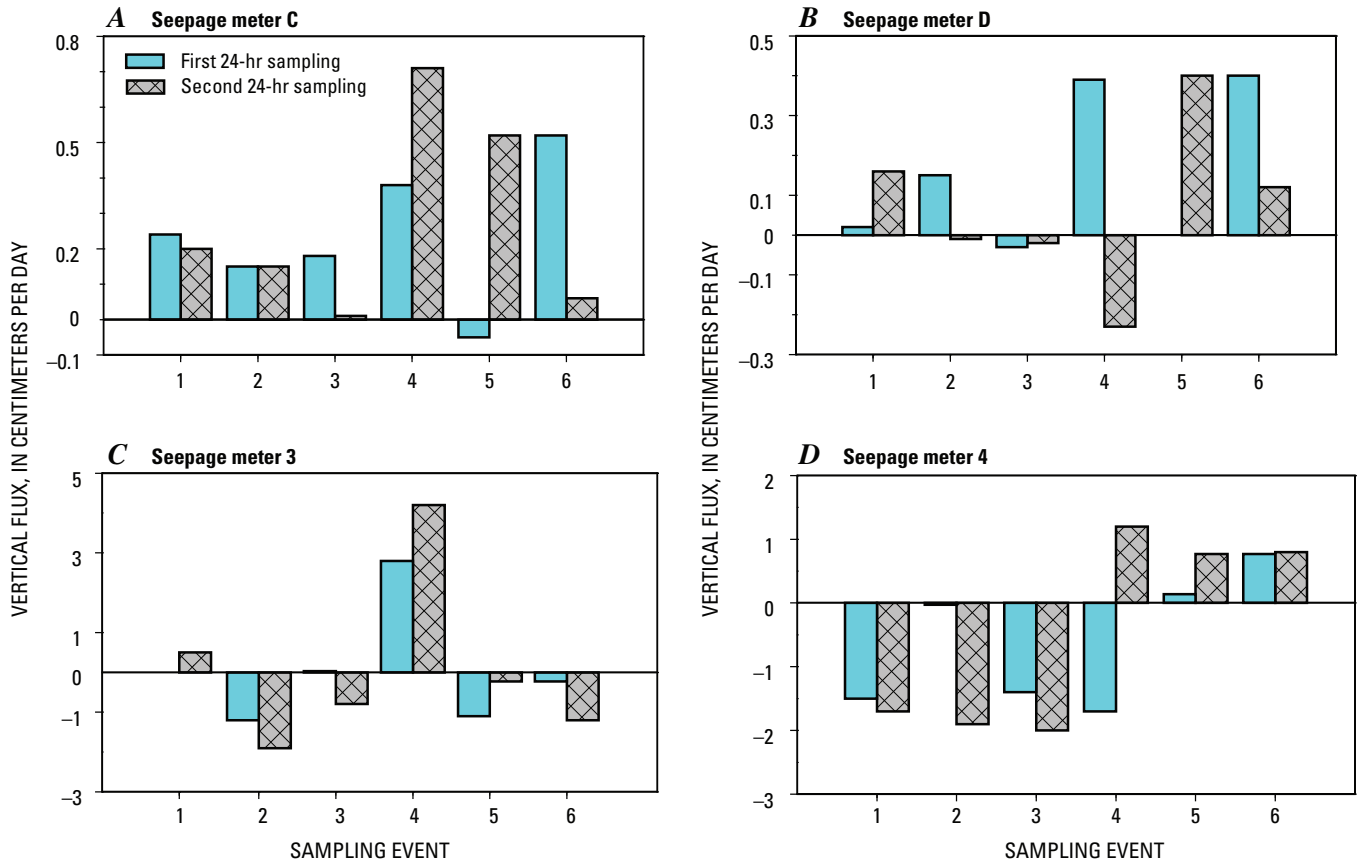
**Figure 9.**    Measured vertical flux rates over consecutive 24-hour measurement periods for seepage meters pairs C-3 and D-4. A. Seepage meter C. B. Seepage meter D. C. Seepage meter 3. D. Seepage meter 4. (hr, hour.)

Four seepage meters were placed in the test tank: two large and two small seepage meters. The system was allowed to equilibrate for 24 hours prior to the tests. The three types of collection bags used were the same as those used in the field (fig. 12). The wall thickness of each of the three collection bags was measured with vernier calipers at 0.41, 0.26, and 0.04 mm, respectively. The collection bags were prefilled with a known volume of water and attached to the seepage meters using a 10-cm length of 0.64-cm-i.d. vinyl tubing. The seepage meters and connected bags were placed in the test tank for 60 minutes for each test run. Seepage meters of the same cross-sectional area were considered pairs for each test run.

Two separate sets of tests were conducted. The objective of the first set of tests (tests 1 through 8) was to compare the results of measured vertical seepage rates with the known vertical test tank seepage rates. For these tests, a packaging bag and a medical bag were connected to the small seepage meters, and a packaging bag and shower bag were connected to the large seepage meters. At the end of a test, the collection bags were disconnected, weighed, and recorded.

The second set of tests (tests 9–12) was conducted using only the packaging bags. The objective of these tests was to evaluate the ability of the collection bag to fill under various test scenarios. The vertical flux rate in the test tank was set to a known constant positive flux rate for the duration of all test runs conducted. The specifics for each of these test runs are presented in the Laboratory Results section.

## Laboratory Results

A relative percent difference (RPD) was used to describe the variability between the measured vertical seepage rates and the known test tank vertical seepage rate for each of the 12 tests. The RPD was calculated as the difference between the measured and known seepage rates divided by the average of the two values and is expressed as a percentage. An RPD of less than 10 percent between the known and measured seepage rates was considered acceptable for the tests conducted in the test tank. Table 3 lists the resulting variability for tests 1–8 in which the performance of the three different bag types was compared with the known test tank vertical flux. The median RPD for the shower bag connected to a large seepage meter was 121 percent, and the median RPD for the medical bag connected to small seepage meters was 96.5 percent. The median RPD for the packaging bags connected to the large and small seepage meters was 13.7 and 7.6 percent, respectively. The results of tests 1 through 8 are depicted as box plots in figure 13.
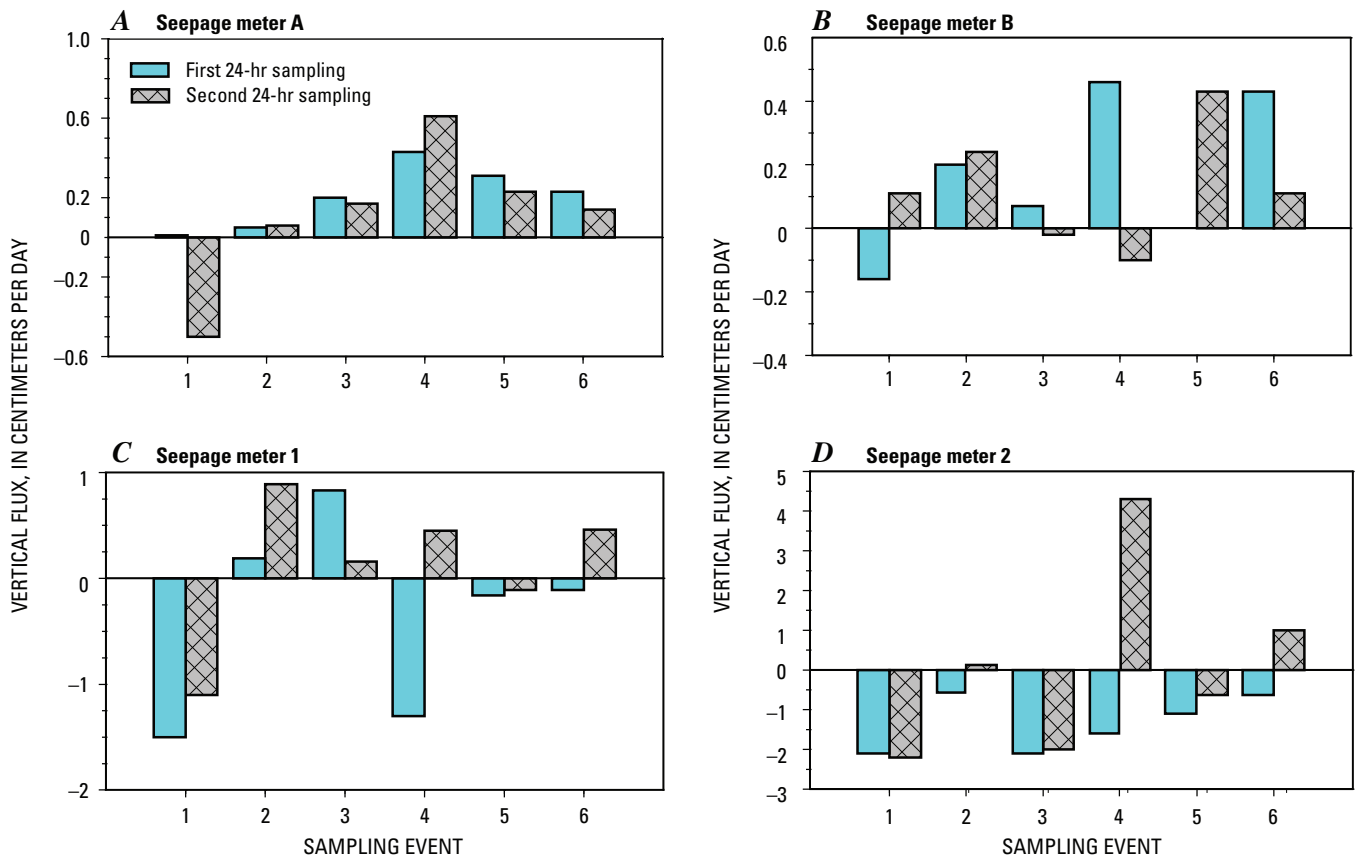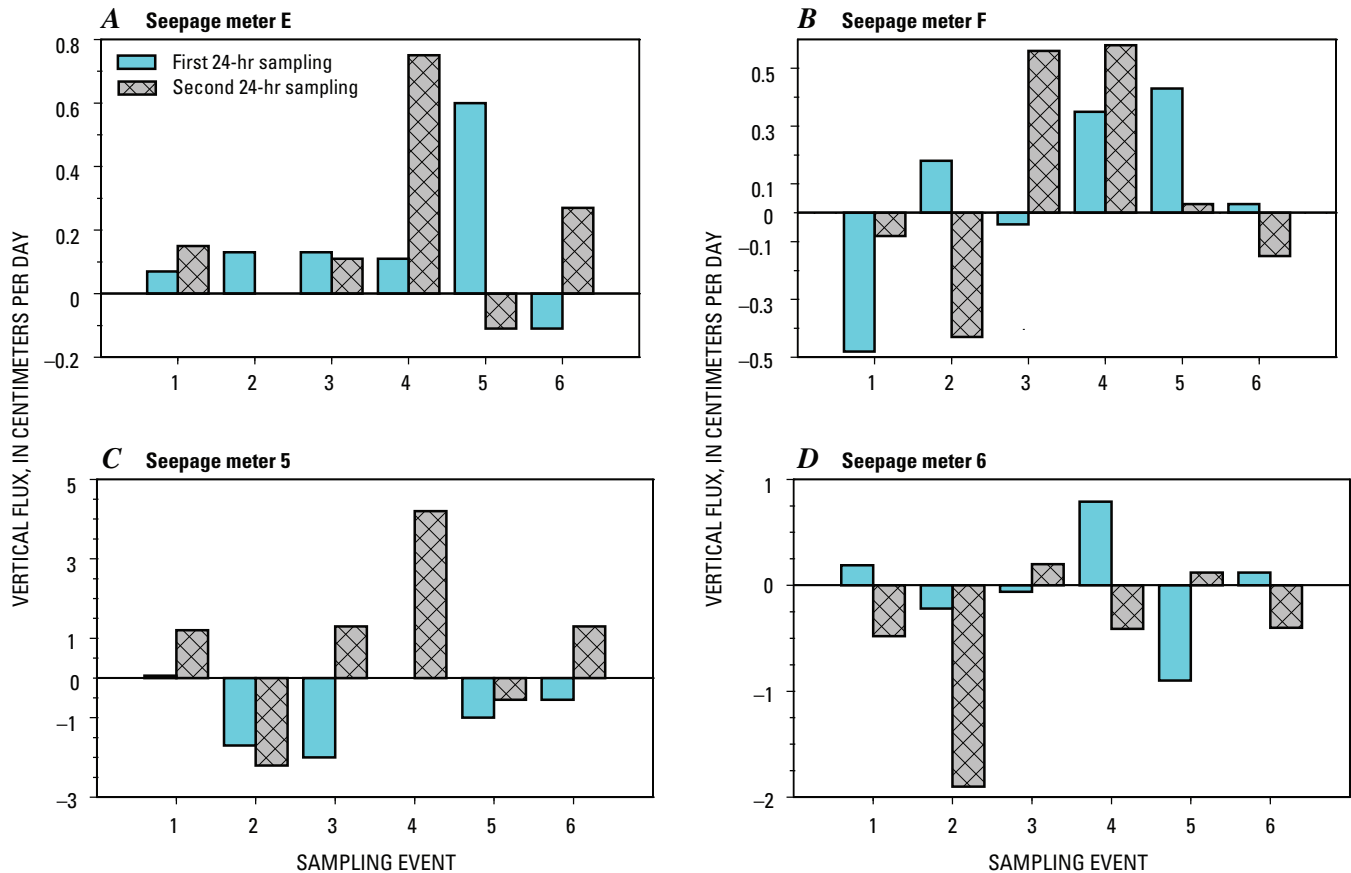
**Figure 10.** Measured vertical flux rates over consecutive 24-hour measurement periods for seepage meter pairs E-5 and F-6. A. Seepage meter E. B. Seepage meter F. C. Seepage meter 5. D. Seepage meter 6. (hr, hour.)

The results from tests 1 through 8 indicate that the thin-walled packaging bags performed better than the thicker-walled collection bags under an applied constant head. The thin-walled bags appear to be more compliant than the thicker-walled bags and filled easily. The compliance of bags to fill under an applied hydraulic head is affected by the size, shape, and the membrane thickness of the bag. The hydraulic head required to cause flow into the collection bags is expected to remain relatively constant until the bags fill with enough water to cause stretching, at which point the volumetric flow into the bag will decrease. Furthermore, if the membrane thickness of the collection bag is too large, the volumetric flow into a bag may reach a point where it rapidly decreases or ceases because the hydraulic head is not enough to overcome the resistance of the thicker-walled bag. Additional hydraulic head would be necessary to overcome the resistance and continue filling the bag. The high RPD for both the medical and shower bags is likely a result of the latter, as the applied constant head during the test runs remained relatively constant throughout each test run, and the collection bags never filled to maximum capacity in any of the test runs. The volumetric flow rate that the flow meter measured at the beginning and end of each test run was recorded, and an RPD was calculated. The RPD between the flow rates at the beginning and end of each test run ranged from 0 to 7.6 percent for all tests (table 4).

In tests 9 through 12, compliance of the thin-walled packaging bags was tested under four different test scenarios (table 5). The results of test 9 indicate that the empty collection bag would fill if the tubing was filled; however, the RPD was twice the acceptable median RPD. Test runs 10 and 11 compare the results starting with a partially filled collection bag and attaching the hose that is filled (test scenario 2) or empty (test scenario 3). In test scenario 3, it was unclear as to whether the applied constant head filled the tubing before flow into the bag occurred, or whether the initial volume that the bag contained filled the tubing to initiate flow into the collection bag. The median RPD for this test scenario was 43.1 percent. The collection bags under test scenario 2 gave the best results. The results indicate that a small initial volume, void of any air bubbles or kinks in the collection bag or tubing, resulted in an average RPD between measured and known flux rates of 6.4 and 5.4 percent for the large and small seepage meters, respectively.

**Figure 11.**    Laboratory test tank setup used for testing of different types of collection bags attached to seepage meters. Test tank setup and design by Michael Menheer in 2004, U.S. Geological Survey  (cm, centimeter; PVC, polyvinyl chloride).



**Figure 12.**    Seepage meter collection bag types. A. Sun Shower Solar Bag. B. medical supply bag. C. Void-Fill packaging bag.

**Table 3.** Results of measured and known vertical flux rates, including relative percent difference, for collection bag types.

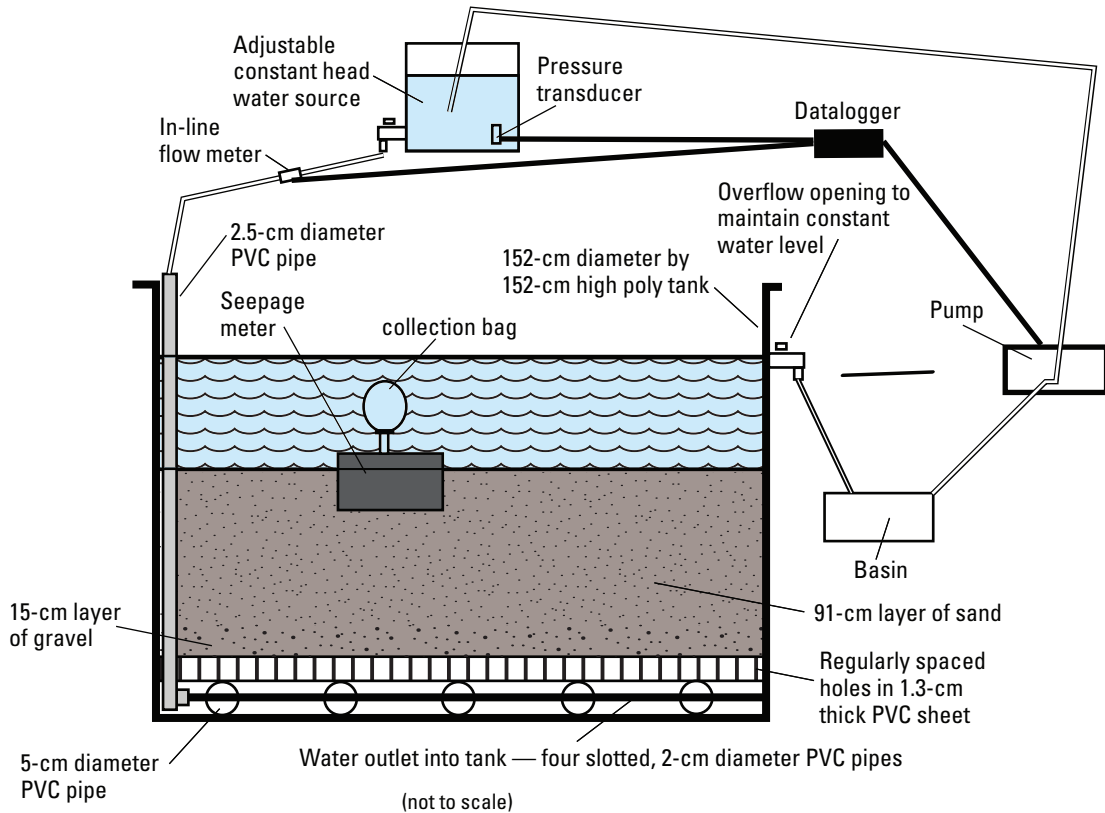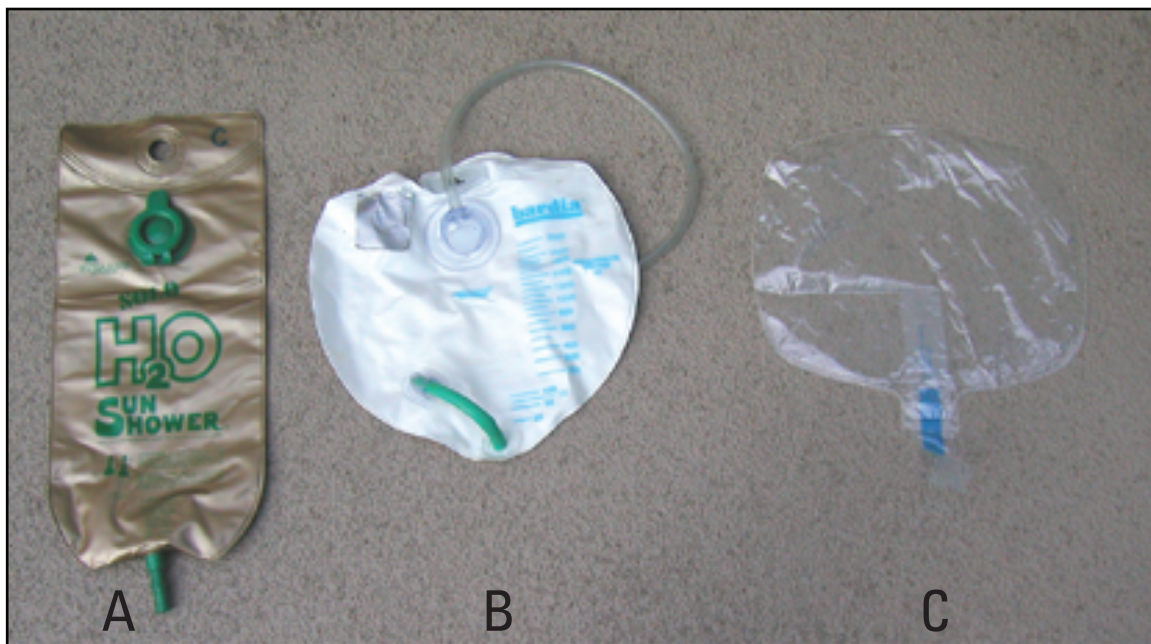[cm, centimeter; NA; not applicable]

| Test number | Seepage meter | Bag type | Measured vertical flux rate (cm/day) | Known test tank vertical flux (cm/day) | Relative percent difference |
|---|---|---|---|---|---|
| 1 | Large seepage meter | shower bag | 3.45 | 17.1 | 133 |
|  | Large seepage meter | packaging bag | setup problem | 17.1 | NA |
|  | Small  seepage meter | packaging bag | 18.5 | 17.1 | 7.66 |
|  | Small  seepage meter | medical bag | 11.6 | 17.1 | 38.4 |
| 2 | Large seepage meter | shower bag | 2.97 | 16.8 | 140 |
|  | Large seepage meter | packaging bag | 14.6 | 16.8 | 13.7 |
|  | Small  seepage meter | packaging bag | 16.3 | 16.8 | 3.02 |
|  | Small  seepage meter | medical bag | 5.65 | 16.8 | 99.1 |
| 3 | Large seepage meter | shower bag | 4.88 | 19.0 | 118 |
|  | Large seepage meter | packaging bag | 16.4 | 19.0 | 14.4 |
|  | Small  seepage meter | packaging bag | 17.7 | 19.0 | 6.81 |
|  | Small  seepage meter | medical bag | 5.46 | 19.0 | 111 |
| 4 | Large seepage meter | shower bag | 3.83 | 17.1 | 127 |
|  | Large seepage meter | packaging bag | 15.1 | 17.1 | 12.8 |
|  | Small  seepage meter | packaging bag | 15.7 | 17.1 | 8.38 |
|  | Small  seepage meter | medical bag | 1.56 | 17.1 | 167 |
| 5 | Large seepage meter | shower bag | 2.57 | 17.1 | 148 |
|  | Large seepage meter | packaging bag | 14.5 | 17.1 | 16.6 |
|  | Small  seepage meter | packaging bag | 18.5 | 17.1 | 7.46 |
|  | Small  seepage meter | medical bag | 4.19 | 17.1 | 121 |
| 6 | Large seepage meter | shower bag | 7.18 | 17.5 | 83.6 |
|  | Large seepage meter | packaging bag | 18.5 | 17.5 | 5.34 |
|  | Small  seepage meter | packaging bag | 15.9 | 17.5 | 9.54 |
|  | Small  seepage meter | medical bag | 10.2 | 17.5 | 52.6 |
| 7 | Large seepage meter | shower bag | 4.02 | 5.21 | 35.5 |
|  | Large seepage meter | packaging bag | 5.65 | 5.21 | 25.7 |
|  | Small  seepage meter | packaging bag | 5.69 | 5.21 | 8.85 |
|  | Small  seepage meter | medical bag | 11.2 | 5.21 | 72.9 |
| 8 | Large seepage meter | shower bag | 2.42 | 5.58 | 79.0 |
|  | Large seepage meter | packaging bag | 5.06 | 5.58 | 9.76 |
|  | Small  seepage meter | packaging bag | 6.00 | 5.58 | 7.23 |
|  | Small  seepage meter | medical bag | 1.95 | 5.58 | 96.5 |

The results of test run 12, in which empty tubing and an empty collection bag were attached to the seepage meters, indicate that the RPD between the known and measured vertical flux rate was much greater than the acceptable difference. The high RPD (median RPD of 90.3 percent) for this test scenario appears to be related to the energy required to open a bag that is initially empty. Other investigators (Erickson, 1981; Shaw and Prepas, 1990a,b; Belanger and Montgomery, 1992; Landon and others, 2001) have reported problems with seepage meter performance when using bags that were initially empty.

Overall, the laboratory results of the three bag types tested indicate that the thin compliant packaging bags performed better than the medical and shower bag under the applied laboratory conditions. In addition, results of test runs 9–12 indicate that the packaging bags performed best when started with an initial volume and filled tubing prior to attachment to seepage meters (test scenario 2). Results of each of the test scenarios summarized in table 5 are depicted in figure 14.
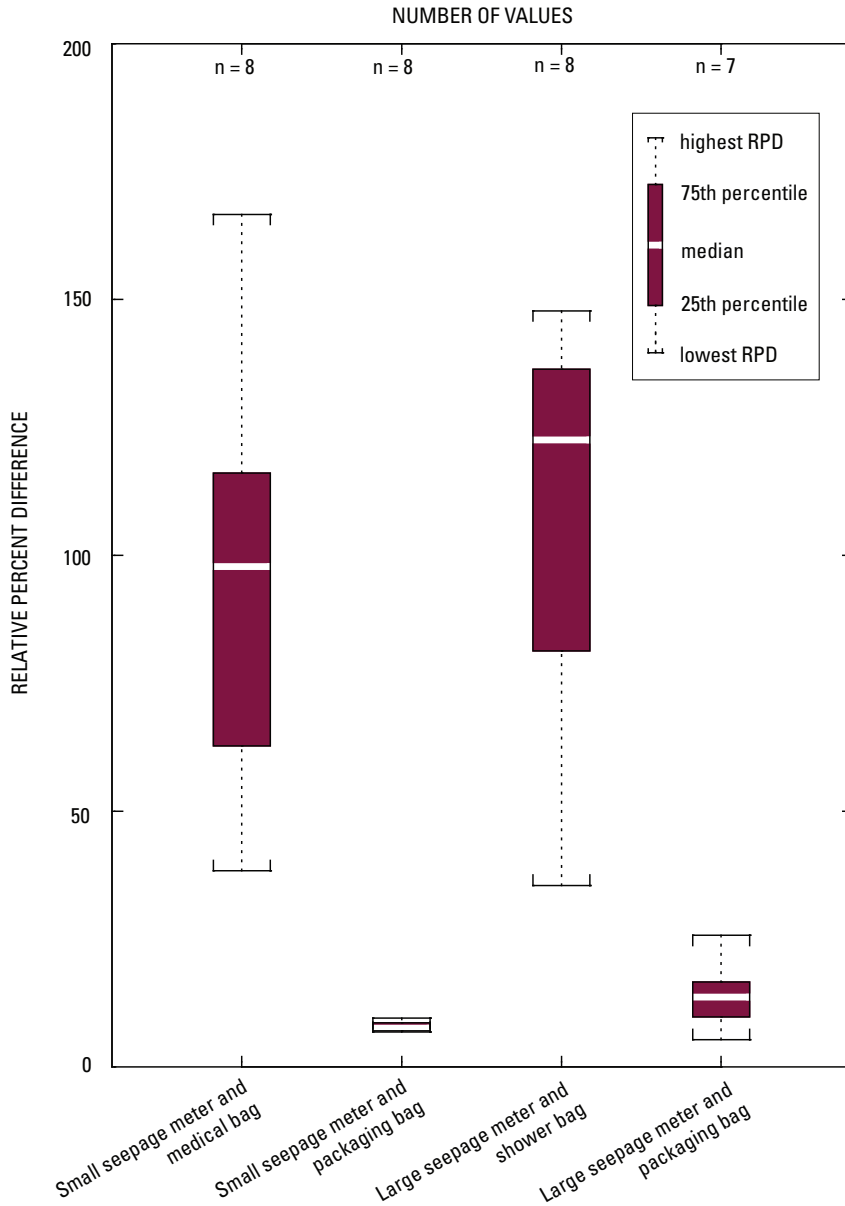
**Figure 13.**    Boxplots of relative percent difference between measured and known seepage rates. (RPD, relative percent difference.)

Laboratory results suggested that use of thin-walled collection bags would provide the best seepage meter results for obtaining streambed fluxes. Following laboratory tests, thin-walled bags were exclusively used as collection bags in the field. All bags were filled with approximately 500 or 1,000 mL of water. The bags were connected to seepage meters with filled tubing, and the water in the bags was void of any air bubbles.

**Table 4.** Comparison of test tank flux rate at beginning and end of each test run.

[mL/min, milliliter per minute]

| Test number | Tank flux rate at start of test (mL/min) | Tank flux rate at end of test (mL/min) | Percent difference |
|---|---|---|---|
| 1 | 219 | 223 | 2.2 |
| 2 | 214 | 209 | 2.2 |
| 3 | 242 | 233 | 3.9 |
| 4 | 219 | 219 | 0.3 |
| 5 | 219 | 204 | 6.5 |
| 6 | 223 | 233 | 4.3 |
| 7 | 66.5 | 67.2 | 1.1 |
| 8 | 71.3 | 71.4 | 0.1 |
| 9 | 233 | 233 | 0.0 |
| 10 | 233 | 233 | 0.0 |
| 11 | 61.7 | 57.0 | 7.6 |
| 12 | 66.5 | 68.2 | 2.6 |

**Table 5.** Results of test scenarios using thin-walled packaging collection bags.

[cm, centimeter; mL, milliliter]

| Test number | Seepage meter | Test scenario description | Test scenario | Measured vertical flux rate (cm/day) | Known test tank vertical flux (cm/day) | Percent difference |
|---|---|---|---|---|---|---|
| 9 | Large | 0 initial volume, tubing filled | 1 | 23.0 | 18.2 | 26.4 |
|  | Large | 0 initial volume, tubing filled | 1 | 22.5 | 18.2 | 23.6 |
|  | Small | 0 initial volume, tubing filled | 1 | 15.2 | 18.2 | 16.5 |
|  | Small | 0 initial volume, tubing filled | 1 | 15.1 | 18.2 | 17.0 |
| 10 | Large | 50 mL initial volume, tubing filled | 2 | 19.5 | 18.2 | 7.1 |
|  | Large | 50 mL initial volume, tubing not filled | 3 | 21.4 | 18.2 | 17.6 |
|  | Small | 50 mL initial volume, tubing filled | 2 | 16.7 | 18.2 | 8.2 |
|  | Small | 50 mL initial volume, tubing not filled | 3 | 11.6 | 18.2 | 36.3 |
| 11 | Large | 50 mL initial volume, tubing filled | 2 | 4.5 | 4.8 | 6.3 |
|  | Large | 50 mL initial volume, tubing not filled | 3 | 7.4 | 4.8 | 54.2 |
|  | Small | 50 mL initial volume, tubing filled | 2 | 4.9 | 4.8 | 2.1 |
|  | Small | 50 mL initial volume, tubing not filled | 3 | 1.8 | 4.8 | 62.5 |
| 12 | Large | 0 initial volume, empty tubing | 4 | 13.8 | 5.2 | 165 |
|  | Large | 0 initial volume, empty tubing | 4 | 13.9 | 5.2 | 167 |
|  | Small | 0 initial volume, empty tubing | 4 | 1.9 | 5.2 | 63.5 |
|  | Small | 0 initial volume, empty tubing | 4 | 2.5 | 5.2 | 51.9 |
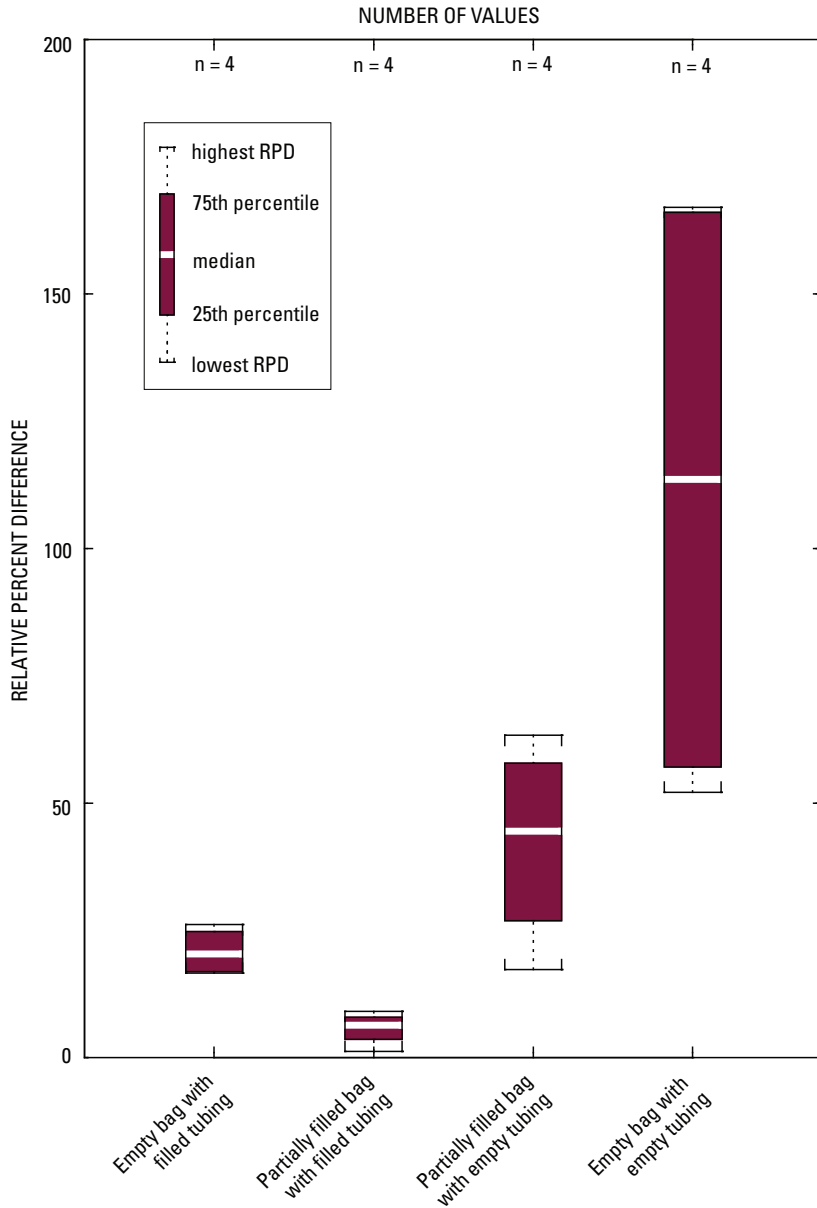
**Figure 14.**    Boxplots of relative percent difference of bag compliance under various test scenarios. (RPD, relative percent difference.)

# Estimates of Streambed Hydraulic Conductivity

Streambed hydraulic conductivity was estimated using grain-size analyses and slug tests. Although slug tests measure hydraulic conductivity values that depend on horizontal and vertical flow, and hydraulic conductivity values from grain-size methods are nondirectional, the two methods are directly compared for the purpose of characterizing streambed hydraulic conductivity.

## Methods

### Grain-Size Analysis

A total of six sediment cores were collected from near each of the in-stream monitoring well pairs depicted in figure 15, and sieve test analysis was conducted on each core. The cores were collected at the sediment–water interface, and the length of collected cores ranged from 25 to 46 cm. Core samples consisted of a homogeneous medium-to-coarse grained, well-sorted sand. The weight percent from each sieve size class was used to calculate a cumulative weight percent, and a grain-size distribution curve was generated for each core collected. The resulting curves depicted in figure 16
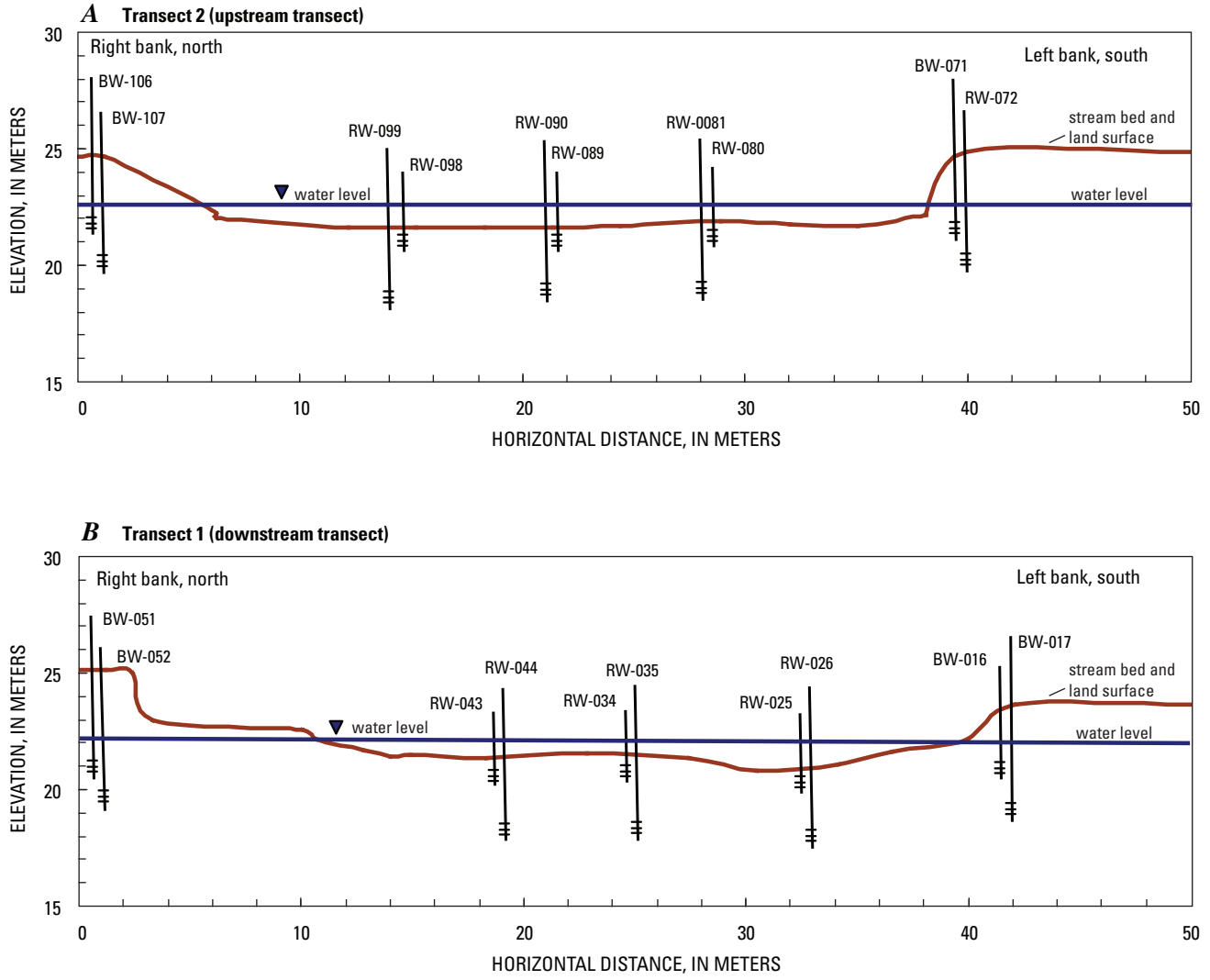
**Figure 15.**   Cross-sectional schematic of monitoring well name and location for the upstream and downstream transects. A. Upstream. B. Downstream. (BW, bank well; RW, river well.)

represent the grain-size distribution curves for the samples collected at the upstream and downstream transects. These curves were used to approximate the hydraulic conductivity of the streambed sediments by the Hazen approximation. This method is applicable to sands where the effective grain size is between approximately 0.1 and 3.0 mm.

## Hazen Approximation

Grain-size distribution curves can be used to estimate the hydraulic conductivity of sands where the effective grain size is between approximately 0.1 to 3.0 mm (Fetter, 2001) by applying the Hazen method (Hazen, 1911). The effective grain size, $d_{10}$, is the size corresponding to the 10 percent line on the grain-size distribution curve and represents passing

of 10 percent finer (by weight) of the sample during the sieve analysis. These values from the generated grain-size distribution curves were applied to the Hazen approximation for hydraulic conductivity as follows:

$$K = C \times (d_{10})^2$$

where:

    $K$ = hydraulic conductivity (cm/s)

    $d_{10}$ = effective grain size (cm/s)

    $C$ = coefficient based on grain size (Fetter, 2001)    (1)

*A*    **Grain-size distribution curve**  transect 2 (upstream transect)



*B*    **Grain-size distribution curve**  transect 1 (downstream transect)
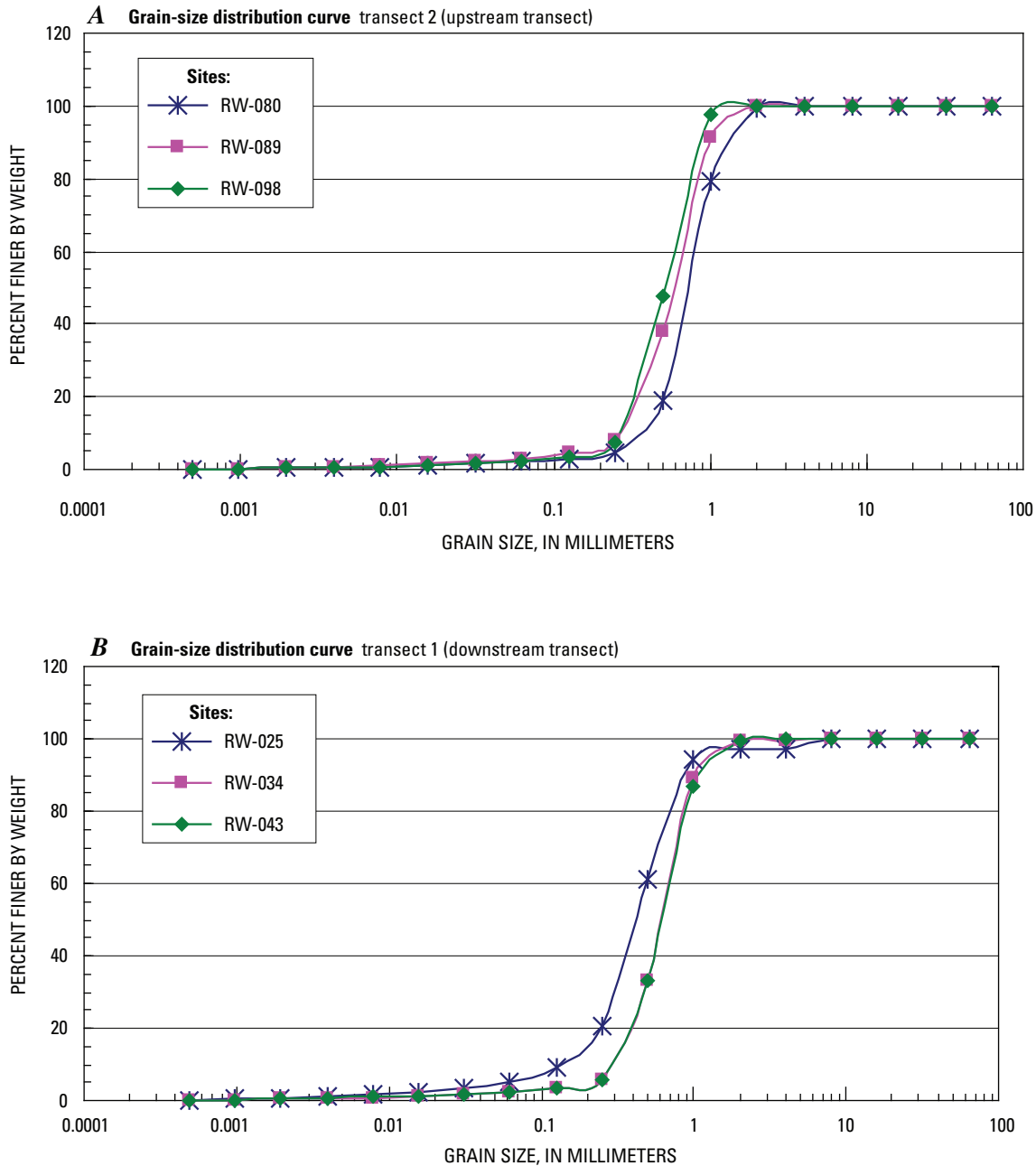
**Figure 16.**    Grain-size distribution curves for sediment cores collected at the upstream and downstream transects.
A. Upstream. B. Downstream. (RW, river well.)

## Slug Tests

Slug tests were performed on 18 of the 20 monitoring wells located at the study site on September 20 and 21, 2004. Eight of the slug tests were performed on the riparian bank monitoring wells screened at approximately 3.5 and 5 m below land surface, and 10 were performed on the in-stream monitoring wells screened at approximately 0.5 and 3 m below the sediment–water interface. Two different slugs were used; both were made of out of PVC plastic tubing,

filled with sand, capped and sealed (dimensions: 45.7 cm by 3.2 cm and 91.4 cm by 3.2 cm, or 1.5 ft by 1.25 in. and 3 ft by 1.25 in.). The larger slug was used in the monitoring wells that were screened at greater depths, and the smaller slug was used in the monitoring wells that were screened at shallow depths. Aquistar PT2X pressure transducers were used to measure and record the head changes during these slug tests. The transducers were set to record at 0.1-second intervals and allowed to equilibrate with the well before the slug was dropped or removed. The recovery time for each
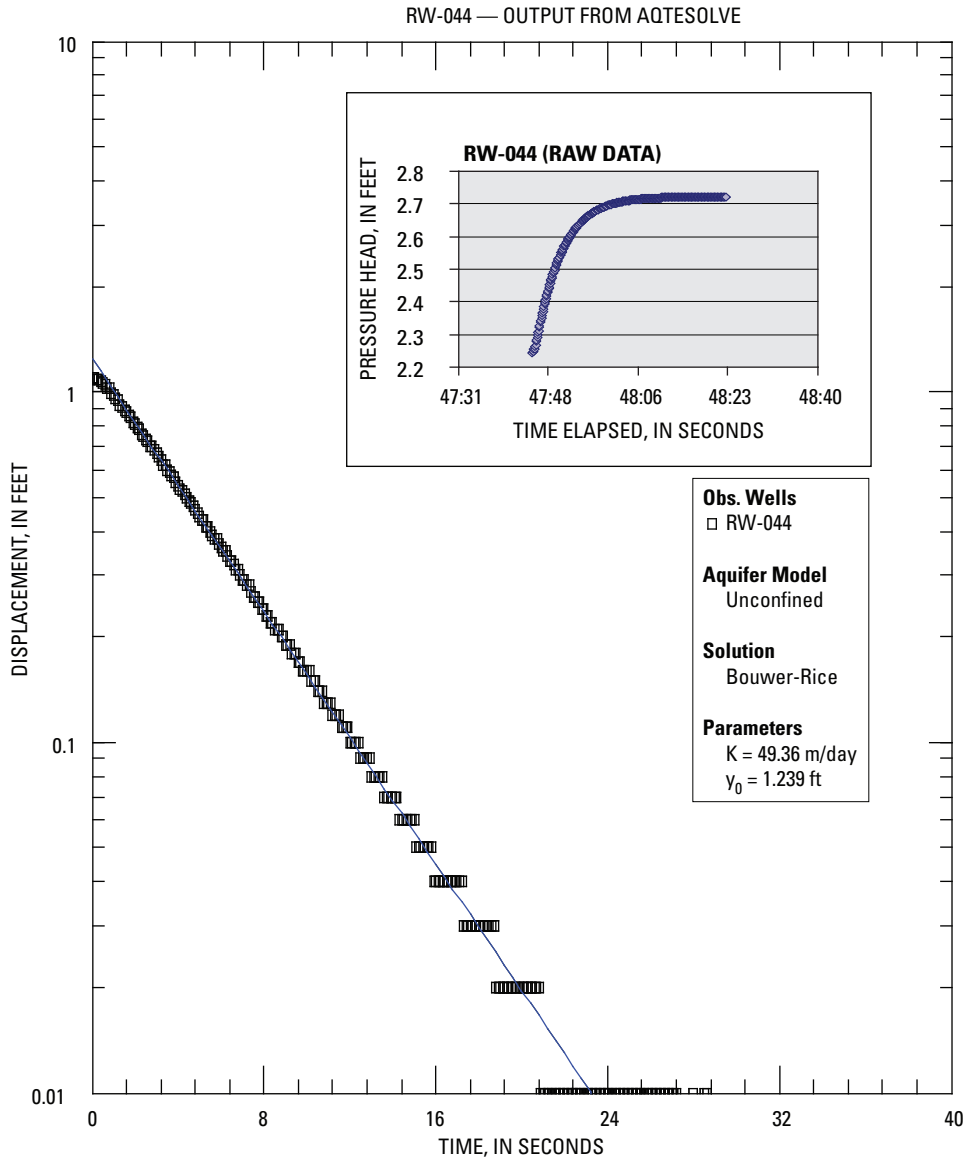
**Figure 17.**   Example of typical recovery time and fit of data for estimating hydraulic conductivity by slug test. (ft, feet; K, hydraulic conductivity; m, meter; Obs., observed; RW, river well.)

individual slug test ranged from seconds to minutes, and only one monitoring well (BW-016) did not fully recover between tests. This well was screened in a silty-clay layer. Figure 17 depicts the typical recovery time and fit of data for estimating hydraulic conductivity.

The Bouwer and Rice (1976) application was used from the AQTESOLV software program to estimate hydraulic conductivity from slug tests. The collected water-level displacement data for each set of slug tests input into the program included only the data beginning with the maximum displacement of water level and assigned time zero. The form factor that AQTESOLV applies to the Bouwer and Rice (1976) solution for an unconfined aquifer assumes the form factor described in Fetter (2001).

## Results

The calculated hydraulic conductivity results of the applied grain-size analysis and slug test method were compared. During low-flow conditions, sediment core samples were collected in August 2004, and slug tests were conducted in September 2004. Sediment core samples used to determine hydraulic conductivity were approximately 25–46 cm in length, and therefore, could be compared with slug tests performed in the shallow in-stream monitoring wells screened at approximately 0.5 m below the sediment–water interface. Estimates of hydraulic conductivity for bank wells are by slug test only, as sediment core samples were not collected for these sites. Tables 6 and 7 present the results of applied methods for the upstream and downstream transects, respectively.

**Table 6.**    Estimated hydraulic conductivity by slug test and (or) grain-size analysis at upstream transect (transect 2).

[Bouwer and Rice = slug test method; Hazen = grain-size method. BW, blank well; ID, identification; m, meter; RW, river well]

| USGS site ID number | Monitoring well ID number | Location and type | Depth | Method of hydraulic conductivity estimate | Measured hydraulic conductivity (m/day) |
|---|---|---|---|---|---|
| 372312120481106 | BW-106 | Bank monitoring well, north bank | shallow | Bouwer and Rice, 1976 | 80 |
| 372312120481107 | BW-107 | Bank monitoring well, north bank | deep | Bouwer and Rice, 1976 | 60 |
| 372312120481098 | RW-098 | River monitoring well, river right | shallow | Bouwer and Rice, 1976 | 120 |
| | | | | Hazen, 1911 | 110 |
| 372312120481099 | RW-099 | River monitoring well, river right | deep | no slug test | no slug test |
| 372312120481089 | RW-089 | River monitoring well, middle | shallow | Bouwer and Rice, 1976 | 50 |
| | | | | Hazen, 1911 | 50 |
| 372312120481090 | RW-090 | River monitoring well, middle | deep | Bouwer and Rice, 1976 | 250 |
| 372312120481080 | RW-080 | River monitoring well, river left | shallow | Bouwer and Rice, 1976 | 50 |
| | | | | Hazen, 1911 | 50 |
| 372312120481081 | RW-081 | River monitoring well, river left | deep | Bouwer and Rice, 1976 | 60 |
| 372312120481071 | BW-071 | Bank monitoring well, south bank | shallow | Bouwer and Rice, 1976 | 40 |
| 372312120481072 | BW-072 | Bank monitoring well, south bank | deep | Bouwer and Rice, 1976 | 40 |

**Table 7.**    Estimated hydraulic conductivity by slug test and (or) grain-size analysis at downstream transect (transect 1).

[Bouwer and Rice = slug test method; Hazen = grain-size method. BW, blank well; ID, identification; m, meter; RW, river well]

| USGS site ID number | Monitoring well ID number | Location and type | Depth | Method of hydraulic conductivity estimate | Measured hydraulic conductivity (m/day) |
|---|---|---|---|---|---|
| 372312120481051 | BW-051 | Bank monitoring well, north bank | shallow | Bouwer and Rice, 1976 | 60 |
| 372312120481052 | BW-052 | Bank monitoring well, north bank | deep | Bouwer and Rice, 1976 | 70 |
| 372312120481043 | RW-043 | River monitoring well, river right | shallow | Bouwer and Rice, 1976 | 100 |
| | | | | Hazen, 1911 | 20 |
| 372312120481044 | RW-044 | River monitoring well, river right | deep | Bouwer and Rice, 1976 | 50 |
| 372312120481034 | RW-034 | River monitoring well, middle | shallow | Bouwer and Rice, 1976 | 30 |
| | | | | Hazen, 1911 | 70 |
| 372312120481035 | RW-035 | River monitoring well, middle | deep | Bouwer and Rice, 1976 | 20 |
| 372312120481025 | RW-025 | River monitoring well, river left | shallow | Bouwer and Rice, 1976 | no slug test |
| | | | | Hazen, 1911 | 70 |
| 372312120481026 | RW-026 | River monitoring well, river left | deep | Bouwer and Rice, 1976 | 40 |
| 372312120481016 | BW-016 | Bank monitoring well, south bank | shallow | Bouwer and Rice, 1976 | 10 |
| 372312120481017 | BW-017 | Bank monitoring well, south bank | deep | Bouwer and Rice, 1976 | 80 |

The estimated hydraulic conductivity for the upstream transect by slug test ranged from 40 to 250 m/day, whereas that for the downstream transect ranged from 10 to 100 m/day. A relative percent difference (RPD) was used to describe the variability in estimates of hydraulic conductivity by grain-size analysis and slug test. Variability in applied methods at the upstream transect ranged from 0 to 9 percent, in which both RW-089 and RW-080 resulted in estimated hydraulic conductivities of 50 m/day. Estimates of hydraulic conductivity for the downstream transect showed greater variability, with a range of 80 to 133 percent between applied methods. Location of screened interval likely explains variability in range of estimates. BW-016 was screened in a silty-clay layer, and pebbles and cobbles were encountered during the installation of the in-stream wells RW-098 and RW-090. The sieve test analysis and slug tests were conducted within one month of each other, and therefore, represent a "snapshot" of hydraulic conductivity during 2004 summer low-flow conditions.

# Estimating Seepage Using Heat as a Tracer

Temperature is a controlling variable for aquatic life in the water column and in streambed sediments. Exchanges that occur between streams and ground-water systems play a key role in controlling temperatures not only in the stream, but also in the underlying sediments. Heat is transported through stream sediments by advection and conduction where temperature differences exist. Heat as a tracer is a simple yet powerful tool for detecting water movement across the sw–gw interface when this movement is traced by continuous monitoring of temperature patterns in the streambed and subsurface water.

The use of heat as a hydrologic tracer has several distinct advantages over applied chemical tracers. The temperature signal occurs naturally, rather than having to be introduced into the stream setting. The primary measurement is temperature, which is robust and a relatively inexpensive parameter to measure. In contrast to chemical tracers, which often require laboratory analysis before interpretation, temperature data are immediately available for inspection and interpretation (Stonestrom and Constantz, 2003). As a result, analyses of subsurface temperature patterns provide information about sw–gw interactions.

Streams exhibit diurnal temperature fluctuations as a result of solar-driven temperature fluctuations at the land surface, whereas ground water is buffered from these temperature fluctuations below the surface. The difference in temperature between streams and ground water provides a means for tracing exchanges between the two systems. In a gaining reach of a river, water is moving upward into the streambed and carries with it the relatively static temperature signal of the ground water. As a result, the temperatures in and beneath the gaining reach are muted compared with the diurnal fluctuations in the stream. Conversely, if the stream is losing water volume by seeping down through riverbed to ground water, and water is moving downward into the streambed, the diurnal temperature signal of the river is carried by advection and conduction into the surrounding sediments. Subsurface temperature patterns will exhibit the diurnal fluctuations seen in the stream. Figure 18 depicts these concepts.

## Review of Literature

Heat has been used as a tracer of subsurface water movement for more than 40 years. Analytical solutions to equations that govern the coupled movement of water and heat have been derived and applied to estimate the rate at which water travels from the surface to great depths (Rorabaugh, 1954; Stallman, 1963). Temperature patterns have also been used to study subsurface flow systems ranging from irrigation water in rice paddies to geothermal water beneath volcanoes (Suzuki, 1960; Sorey, 1971). Lapham (1989) used annual temperature records from deep observation wells to identify rates of vertical water flux in several streams in Massachusetts and New Jersey that were based on analytical solutions reported in earlier work (Lapham, 1988). However, these analytical solutions were derived for a few idealized cases and resulted in theoretical, rather than practical, applications because of measurement and computational limitations. Recently, the measurement and modeling of heat and water transport have benefited from significant improvements. Recent innovations in sensor and data-acquisition technology, along with substantial improvements in numerical modeling, present new opportunities for the use of heat as a tracer of stream–ground water exchanges (Stonestrom and Constantz, 2004). Inexpensive and accurate devices are now available for measuring temperature, water level, and water content. These devices, in conjunction with currently available numerical models, provide general solutions of equations for the coupled transport of heat and water.

Sw–gw exchanges can be estimated using heat as a tracer in conjunction with water level measurements (Silliman and Booth, 1993; Silliman and others, 1995; Stonestrom and Constantz, 2003; Anderson, 2005). Temperature has been used as a tracer to identify vertical flux across the sw–gw interface at various locations in the United States. In the Rio Grande near Albuquerque, New Mexico, Bartolino and Niswonger (1999) used the USGS numerical model (VS2DH) to match simulated temperature data to observed temperature, yielding predicted estimates of deep streambed fluxes and spatially averaged hydraulic conductivities. Application of heat as a tracer has been used to examine interactions in alpine streams between stream temperature, streamflow, and ground-water exchanges (Constantz, 1998). The analysis of temperature profiles in ephemeral stream environments has been used to examine percolation characteristics beneath arroyos in the Middle Rio Grande Basin, New Mexico (Constantz and Thomas, 1997), to determine streamflow frequency and duration (Constantz and others, 2001), and to investigate stream losses beneath ephemeral channels (Constantz and others, 2002). Stonestrom and Constantz (2003) provide technical details of the use of heat as an environmental tracer as well as a compilation of seven detailed case studies that use temperature patterns and their interpretation as a hydrologic tool for the assessment of interactions between surface water and ground water in a variety of environmental settings throughout the western United States.
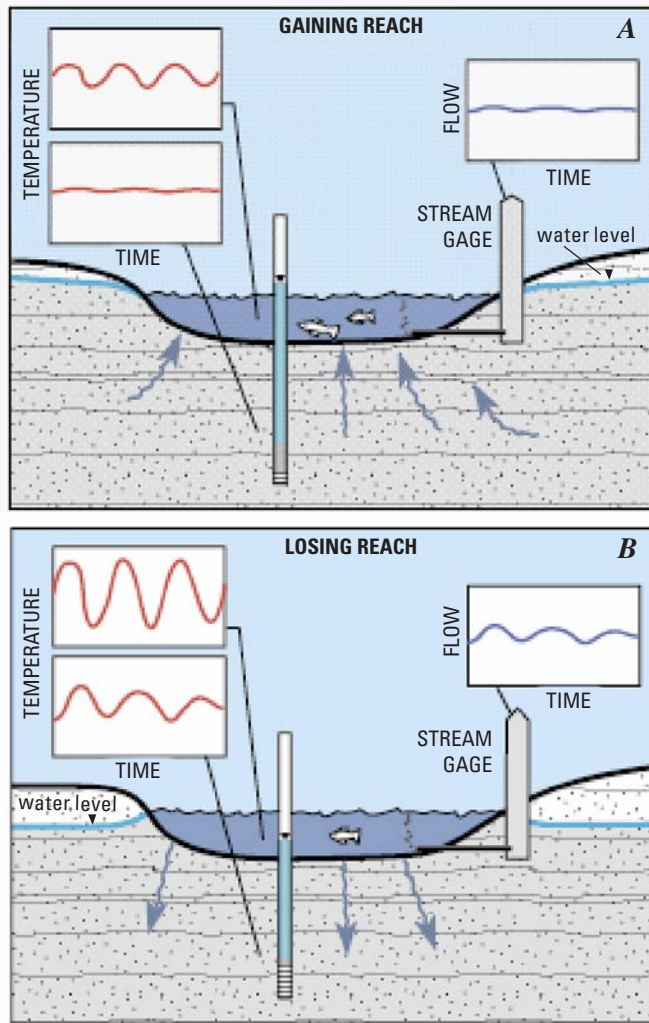
**Figure 18.**    Streamflow and temperature histories for gaining and losing reaches of a stream coupled to the local ground-water system. Ground water is buffered from temperature fluctuations at the land surface.  A., temperature fluctuations in and beneath the gaining reach are therefore muted (top panel) compared with B., temperatures in and beneath the losing reach (bottom panel). Modified with permission from Stonestrom and Constantz, 2004.

## Sampling Design and Methodology

The study site location on the lower Merced River was selected because the reach was within the study area that encompassed the overall USGS's NAWQA agricultural chemical transport (ACT) study design and objectives. To understand how agricultural chemicals move through and between hydrologic compartments (atmosphere, surface water, the unsaturated zone, ground water, and sw–gw interaction), a gaining reach of river was preferable for the sw–gw component. Reconnaissance of the reach indicated that the reach was gaining and easily accessible for sampling equipment installation and subsequent sampling events. In addition, agricultural chemicals of interest were being applied to crops north and south of the selected reach.

A total of twenty 5-cm (2 in.) polyvinyl chloride (PVC) screened monitoring wells were installed across two transects in the Merced River. Transects were separated by a distance of approximately 100 m. Each transect was equipped with five pairs of monitoring wells: three pairs in the river and a pair on the right and left banks in the riparian zone. Figure 19 depicts a bank and in-stream monitoring well pair. The pairs of monitoring wells at each transect consisted of a shallow and a deep monitoring well screened at approximately 0.5 and 3 m below the streambed for the in-stream monitoring wells, and at approximately 3.5 and 5.0 m below the top of well casing for the riparian zone monitoring wells. The monitoring wells were equipped with temperature loggers and pressure transducers. Figure 20 depicts a cross-sectional view of an equipped transect.

Temperature loggers monitored temperature continuously in both the surface water (above the sediment–water interface) and at three depths within the streambed at both transects. Pressure transducers located in the stream and below the streambed collected water-level data that were used to define boundary conditions. Temperature and pressure-head data were input into the USGS numerical model, Variably Saturated 2-Dimensional Heat (VS2DH; Healy and Ronan, 1996) and its graphical interface VS2DI (Hsieh and others, 2000). This program uses an energy transport approach via the advection–dispersion equation to simulate heat and flow transport. Estimates of streambed hydraulic and thermal conductivity were input into the model until model simulations "fit" observed subsurface streambed temperatures. This inverse modeling method uses a visual best fit and is most sensitive to variations in the input parameter K (hydraulic conductivity).

The monitoring wells were installed by pumping the streambed sediment out while pushing in a 15-cm (6 in.) diameter PVC casing downward to the desired depth. After reaching the desired depth, the smaller 5-cm (2 in.) PVC monitoring well was inserted inside the 15-cm PVC casing, and the 15-cm casing was pulled out of the streambed, allowing the surrounding streambed sediments to collapse around the 5-cm PVC monitoring well. The streambed monitoring wells were installed so that the top of the casing of each of the wells was slightly above the streambed. Once in place, the monitoring wells were sealed with standard pressurized monitoring well caps to prevent stream water from entering the monitoring wells. The same installation procedure was used for the riparian zone monitoring wells; however, a combination of hand augering and pumping was used to install the outer casing to the desired depth. A Monterey sand pack was placed around the screened interval of each of the riparian zone monitoring wells. The wells were then sealed with a bentonite cap and backfilled to land surface. Convection in the riparian zone wells was not of concern because convection does not occur in small-diameter wells under saturated conditions or in the absence of large temperature gradients between temperature probes, as confirmed by reconnaissance and collected data.
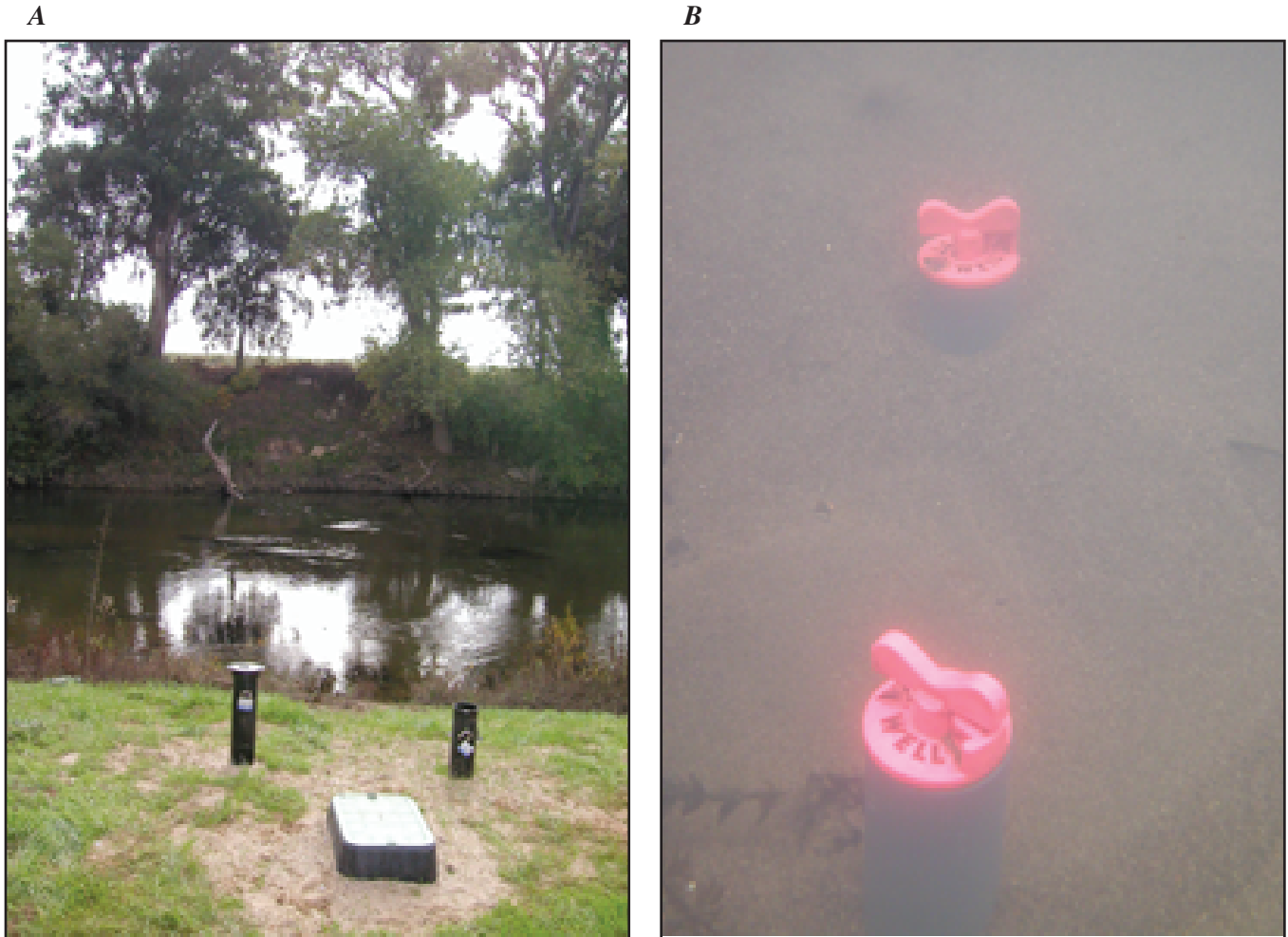
*A*

*B*



**Figure 19.**   Bank and in-stream monitoring well pair at downstream transect. A. Bank. B. In-stream. The center rectangular object is a cover for the tubing that was used to sample wells.

A string of three HOBO Water Temp Pro temperature loggers (accuracy: ±0.2°C at 0 to 50°C range) was fastened to a small diameter rope at depths of approximately 0.5, 1.0, and 2.0 m from the monitoring well cap (fig. 21). These depths were chosen because during reconnaissance of the site, static ground-water temperatures were encountered at approximately 2.5 m below the sediment–water interface. The temperature loggers were then weighted with a stainless-steel bolt and placed in each of the deep in-stream monitoring wells. The same procedure was used for the riparian zone monitoring wells; however, the temperature loggers were placed at approximately 3.5, 4.0, and 5.0 m below the top of the monitoring well casing. These depths were chosen because the water table was approximately 3 m below land surface. A temperature logger was also placed in the stream to record stream temperature. A total of 10 pressure transducers were

used to record water levels: eight in four pairs of the in-stream monitoring wells, one in the deep riparian monitoring well at the downstream transect, and one in the Merced River.

Temperature and pressure were measured at 15-minute intervals. Manual water level measurements were also taken through the study in the riparian zone monitoring wells and during data downloads for the in-stream monitoring wells. Because the top of the casing for the in-stream monitoring wells was underwater (approximately 5–10 cm above the streambed), a 1.8-m riser was attached to the in-stream monitoring well and allowed to equilibrate prior to water level measurements. Table 8 identifies the wells by name, location, and the type of continuous data (temperature and [or] pressure head) recorded in each of the monitoring wells.
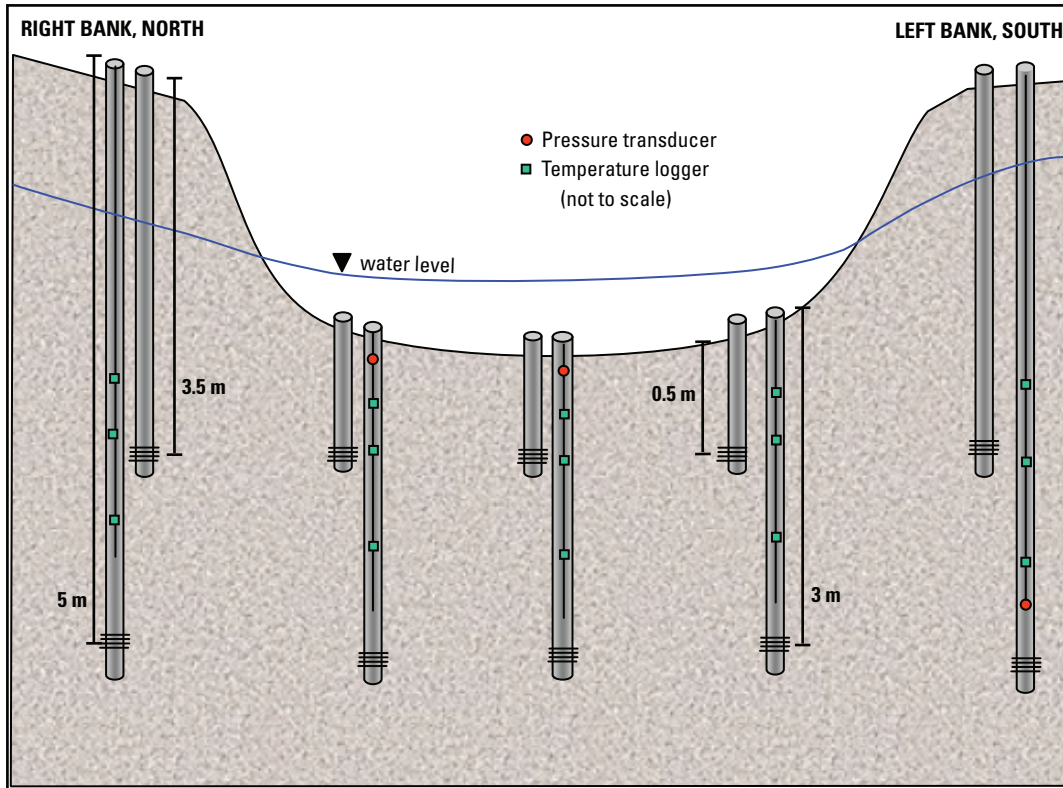
**Figure 20.** Cross-sectional view of instrumented transect. (m, meter.)

## Results

In this study, the application of temperature as a tracer utilized continuous monitoring of water levels, and subsurface temperature, as well as the elevation and temperature of the stream. Data were used to specify the boundary conditions in the numerical model VS2DH, and estimates of hydraulic and thermal conductivity were adjusted in the model until "best fit" simulations matched the observed subsurface stream temperatures at intermediate depth. This method requires high precision in the water-level data and certainty in the elevations (depths) at which the pressure transducers are placed at. However, because of problems associated with the instrumentation used to record continuous water-level elevation, prolonged unexpected high streamflow events, and the resulting scour and burial of the monitoring wells, the results of the recorded total-head distributions and temperature profiles are discussed prior to the modeling results, as these results affect the final model results. Furthermore, results and discussion of total-head distributions and collected temperature data for monitoring wells at the upstream transect are not presented because of vandalism and scour.

## Total-Head Distributions

Total hydraulic head (meters) is defined as the recorded pressure head plus the known elevation at which each of the pressure transducers was placed. A pressure transducer was placed in the river to record continuous stream elevation data. These recorded stream elevations were used to calculate differences in total head between the ground water and the river, thereby indicating the direction of flow across the sediment–water interface at the instrumented site. Gaining and losing reaches were defined from the perspective of the river, which is standard protocol. Specifically, a positive value indicates a gaining reach and a negative value indicates a losing reach. However, in the present study, the pressure transducer placed in the river did not provide the quality of data that the instrument was intended to record for several reasons. The initial study design included a plan for differences in head between the river and ground water on a very small scale (1–3 cm). Unfortunately, the inherent error associated with the estimated elevation of the location of the pressure transducer placed in the Merced River was greater than the measured head differences between the surface water and ground water. This problem was further complicated with each download of data; when the pressure transducer was removed and downloaded, it was nearly impossible to replace the instrument at an exact height in the well. In addition,
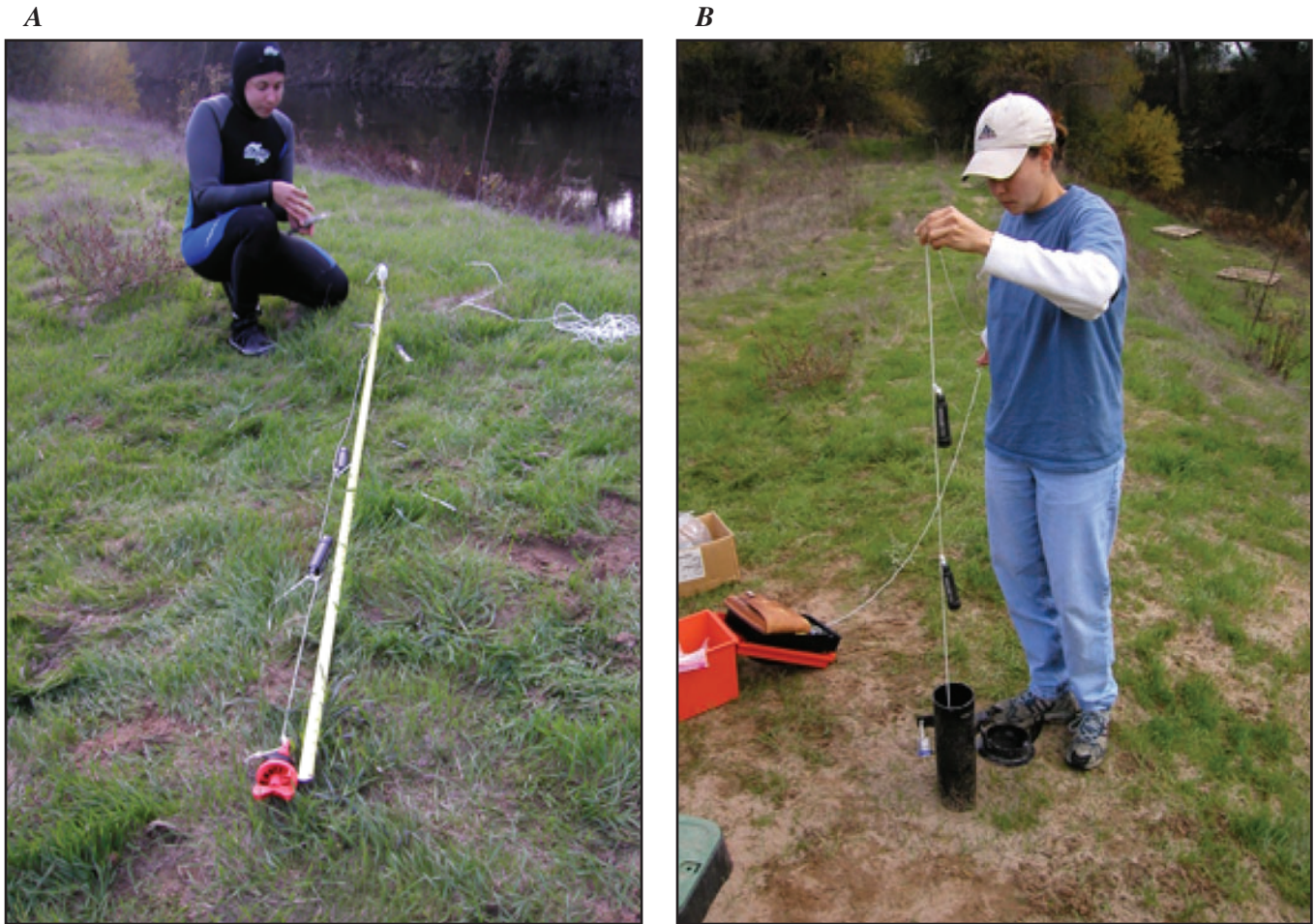
A

B



**Figure 21.** Measurement of spacing for temperature loggers placed in in-stream well and placement of temperature loggers in riparian bank well. A. In-stream well. B. Riparian bank well.

the PVC casing that housed the pressure transducer was at approximately a 40° angle from horizontal, and it was difficult to replace the instrument at its intended location because it was not free-hanging under gravity.

Pressure transducers located below the streambed in the paired monitoring wells screened below the streambed did not have these limitations. These pressure transducers were attached to the cap of the monitoring wells and allowed to hang freely within the monitoring well. Manual water-level measurements taken immediately after data downloads agreed well with recorded water levels to within <0.3 cm. As a result, the paired in-stream monitoring wells (MW) (delta H = deep MW – shallow MW) were used to calculate head differences.

Although the pressure head recorded in each of the streambed monitoring wells agreed with manual measurements, the minor discrepancy between the recorded water level and measured water level seemed to increase in the latter part of the study, suggesting drift in the pressure transducers. The pressure transducers used in this study were not vented to the atmosphere and were placed in monitoring wells that were sealed at the streambed. As a result, this type of pressure transducer requires an additional pressure transducer

(baro-logger) to record and compensate for changes in atmospheric pressure. The data collected from the baro-logger were subtracted from the recorded head data collected in the monitoring wells. The atmospheric pressure and water levels calculated by the baro-logger and the pressure transducers are temperature compensated, though large changes in temperature over a short period can affect how the instrument calculates water pressure (Davies, 2002).

Figure 22 depicts discharge and recorded head differences (delta H) between the deep and shallow monitoring wells at the downstream transect. Mean daily discharge data is obtained from the Department of Water Resources stream gaging station, Merced River near Stevinson (site ID 11272500), approximately 16 mi upstream from the study area. An 18-hour travel time was determined and applied using a travel-time equation from Kratzer and Biagtan (1997). The pressure transducer malfunctioned after the September 2004 download in monitoring well pair RW-044 and RW-043 (fig. 22A). Head differences for monitoring well pair RW035 and RW034 (fig. 22B) recorded a generally gaining river throughout the study period with distinct flow reversals (gaining to losing) during high streamflow events. These

**Table 8.**    Monitoring well identification number, depth, location, and type of data collected.

[BW, blank well; ID, identification; RW, river well]

| USGS site ID number | Monitoring well number | Screened depth (meters) | Transect | Equipment[1] |
|---|---|---|---|---|
| 372312120481106 | BW-106 | 3.5 | upstream, transect 2 | none |
| 372312120481107 | BW-107 | 5 | upstream, transect 2 | temperature loggers |
| 372312120481098 | RW-098 | 0.5 | upstream, transect 2 | pressure transducer |
| 372312120481099 | RW-099 | 3 | upstream, transect 2 | temperature loggers and pressure transducer |
| 372312120481090 | RW-090 | 0.5 | upstream, transect 2 | pressure transducer |
| 372312120481089 | RW-089 | 3 | upstream, transect 2 | temperature loggers and pressure transducer |
| 372312120481080 | RW-080 | 0.5 | upstream, transect 2 | temperature loggers |
| 372312120481081 | RW-081 | 3 | upstream, transect 2 | none |
| 372312120481071 | BW-071 | 3.5 | upstream, transect 2 | none |
| 372312120481072 | BW-072 | 5 | upstream, transect 2 | temperature loggers |
| 372312120481051 | BW-051 | 3.5 | downstream, transect 1 | none |
| 372312120481052 | BW-052 | 5 | downstream, transect 1 | temperature loggers |
| 372312120481043 | RW-043 | 0.5 | downstream, transect 1 | pressure transducer |
| 372312120481044 | RW-044 | 3 | downstream, transect 1 | temperature loggers and pressure transducer |
| 372312120481034 | RW-034 | 0.5 | downstream, transect 1 | pressure transducer |
| 372312120481035 | RW-035 | 3 | downstream, transect 1 | temperature loggers and pressure transducer |
| 372312120481025 | RW-025 | 0.5 | downstream, transect 1 | none |
| 372312120481026 | RW-026 | 3 | downstream, transect 1 | temperature loggers |
| 372312120481016 | BW-016 | 3.5 | downstream, transect 1 | none |
| 372312120481017 | BW-017 | 5 | downstream, transect 1 | temperature loggers and pressure transducer |

[1]Additional information in table 1.

flow reversals correspond to storm events during winter months, relatively large releases at the New Exchequer Dam to improve downstream salmon habitat from mid-April to mid-May, and smaller releases made in October as part of the Vernalis Adaptive Management Plan (VAMP). The water-level data collected from the monitoring well pair RW044 and RW043 (fig. 22A) did not record a flow reversal across the sediment–water interface during the May 2004 VAMP release.

Agricultural fields upgradient of the transects are irrigated between March and September, which seasonally recharges the surficial aquifer. The rise in water levels of the surrounding aquifer is reflected in the water levels of the monitoring well pairs, indicating a gaining stream during irrigation season 2004. Irrigation season 2005 did not result in gaining conditions because of large streamflow releases from New Exchequer Dam beginning March 2005 and continuing through the end of the study period. These releases were made as a result of spring melt of an exceptionally high snowpack in the upper part of the basin.

## Temperature Profiles

During the winter months, the stream temperature becomes much cooler than recorded subsurface temperatures, and conversely during the summer months, the stream temperature becomes much warmer. Figure 23 depicts daily average temperature profiles collected at the downstream transect. The in-stream monitoring wells recorded nearly the same temperature patterns at 0.5, 1.0, and 2.0 m below the streambed. Periods of gaining or losing are recorded, and in general, the subsurface temperatures indicate a slightly gaining-to-neutral reach throughout 2004, with the exception of mid-April to mid-May 2004 during the VAMP flow events when the temperature record indicated a losing scenario.

Temperature records from 2005 coincide with the exceptionally high streamflow. This likely caused scour around the in-stream monitoring wells during the rising limb of the hydrograph and subsequent burial during the falling limb. Field observations support this assumption. As a result, significant uncertainty was created with respect to depth of recorded temperature variations. Despite this concern, the collected temperature data for this time period indicates a losing-stream scenario until June 2005, after which a strongly gaining-stream time period is recorded. Stream elevation approached and overtook bank well BW017 during the spring 2005 dam release and was in direct contact with the river and recorded stream temperature.

The bank wells follow the same temperature patterns as the in-stream wells, but to a much lesser extent. During the summer months, ground-water temperatures at 3.5 m were warmer than those recorded at 5 m, and conversely, during the winter months, recorded temperatures at 5 m were warmer than those at 3.5 m. These changes occurred in June and November, respectively. The bank wells do not record diurnal temperature variations (fig. 24), but do record slight seasonal changes.
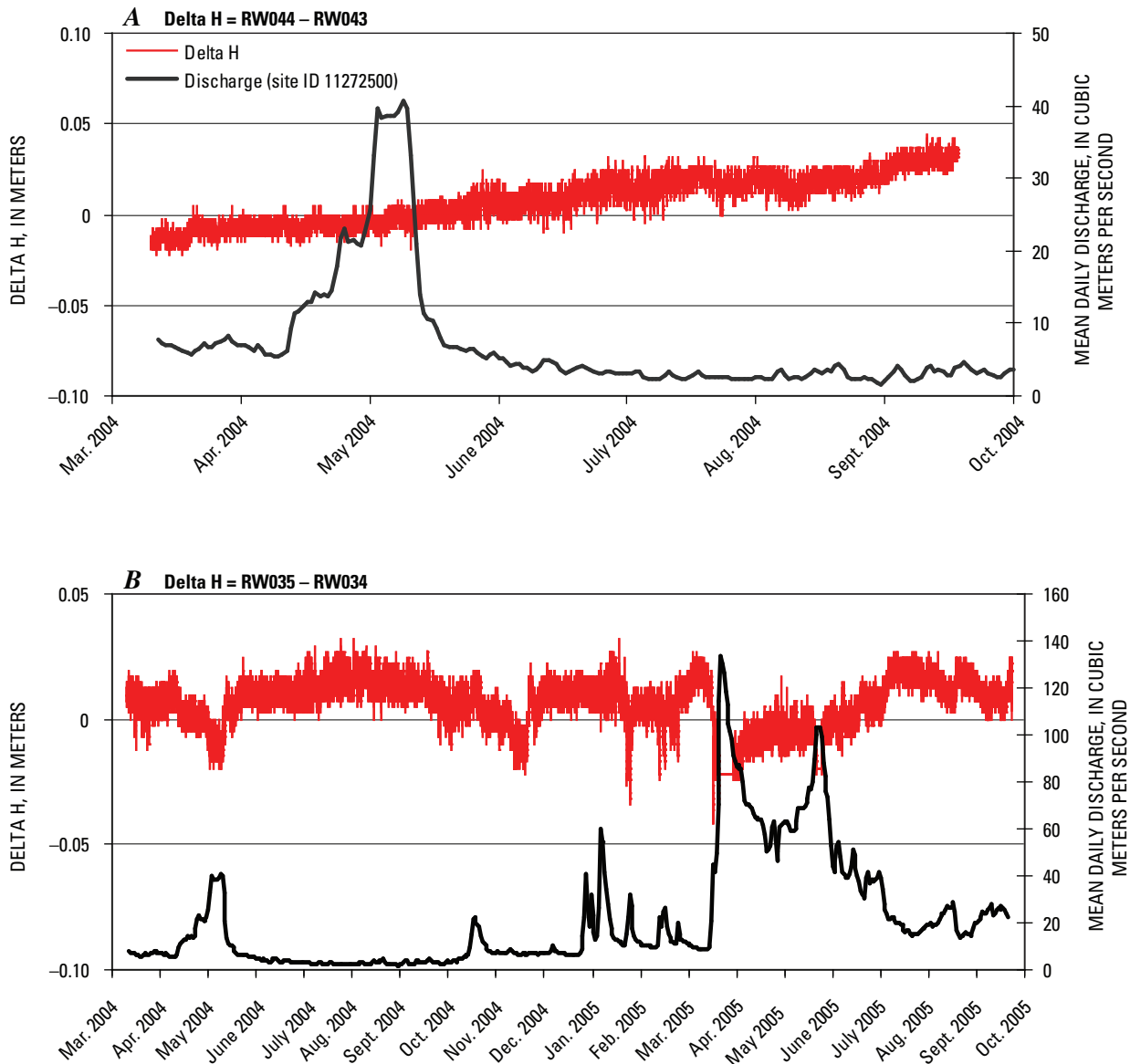
**Figure 22.** Head differences (delta H) between deep and shallow well pairs.  A. Deep pair RW044–RW043. B. Shallow pair RW035–RW034. (delta H, water level difference between the deep and shallow monitoring wells. ID, identification; no., number; RW, river well.)

## Flux Estimates from Heat- and Water-Flow Model Analyses

One-dimensional modeling of heat and water flow was used to interpret temperature and head observations and to estimate vertical sw–gw fluxes at wells RW044 and RW035 in the downstream transect. Two vertical, one-dimensional models with 2-cm grid-blocks were calibrated for each of the deep monitoring wells at the downstream transect, and each well was modeled separately (fig. 25).

The energy transport and water-flow model, VS2DH, was used to fit simulated temperatures to observed temperatures and heads. At the beginning of the study, the intention was to apply recorded pressure head of the surface water to the top boundary and pressure head of the deep monitoring wells to the bottom boundary of each of the one-dimensional models. However, because of issues with the quality of data of the surface-water pressure transducer as discussed in the total-head distribution section, a new approach to applying pressure-head data to the model was necessary.
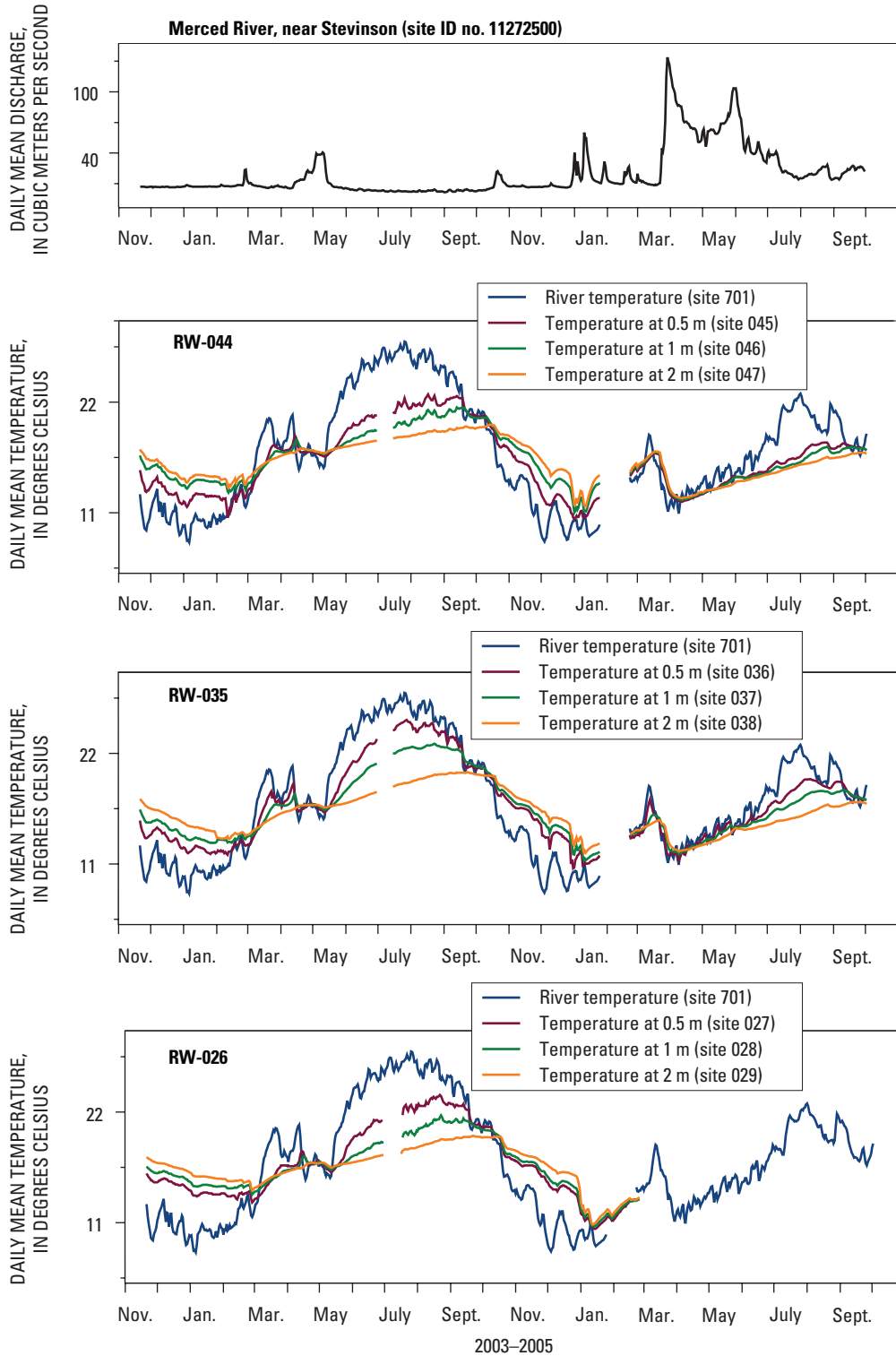
**Figure 23.**   Temperature profiles collected at instrumented in-stream monitoring wells at the downstream transect (transect 1) during the study period.  The line breaks on the graph represent missing data. The three digit site number in the figure legend refers to the USGS site identification number with reference to figure 2 and table 1. (ID, identification; m, meter; no., number; RW, river well; USGS, U.S. Geological Survey.)
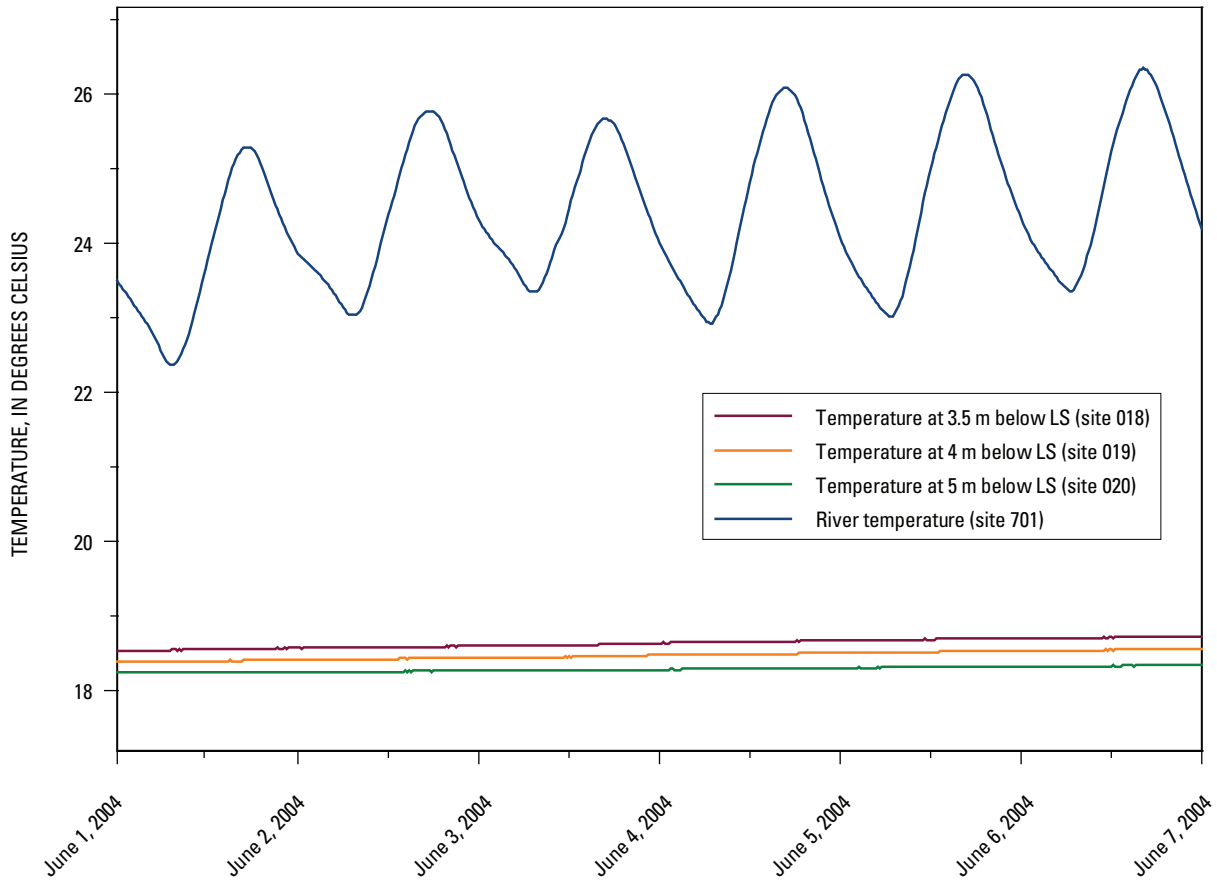
**Figure 24.** Diurnal scale of temperature profile for monitoring well BW-017 during June 2004. The three digit site number in the Figure legend refers to the USGS site identification number with reference to figure 2 and table 1. (LS, land surface; m, meter; USGS, U.S. Geological Survey.)
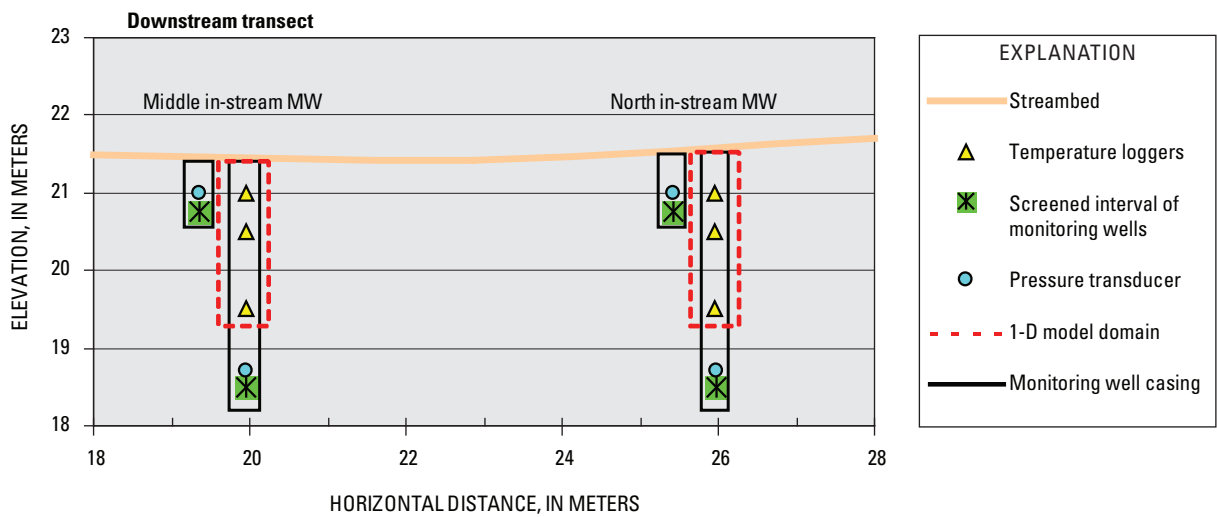


**Figure 25.** Cross-section of downstream transect (transect 1) showing measurement locations and model domain. (D, dimensional; MW, monitoring well.)

The difference in pressure head between the deep and shallow wells was assigned to the bottom boundary, and a pressure head of 0 was assigned at the sediment–water interface (top boundary) for the model. Positive pressure heads indicate discharge from the aquifer to the stream. Figure 25 depicts the model domain at 2 m below the streambed, with a lower model boundary that corresponds to the deepest temperature logger; however, the screened interval of the MW is at 3 m below the streambed. As a result, the head difference between a deep and shallow well is over a vertical distance of 2.5 m and does not match the model domain. It was assumed that the measured head difference over 2.5 m was linear and that K of the materials throughout the model domain was constant as a result of the homogenous streambed material. Therefore, the head difference over 2.5 m was corrected to a head difference over 2 m to match the model domain.

The temperatures applied to the top and bottom boundaries were recorded above the sediment–water interface and 2 m below the streambed, respectively. Estimates of streambed hydraulic conductivity were input into the model until model simulations provided a "best fit" of observed temperatures at depth. The observed temperatures used to match model simulations were measured were 0.5 and 1.0 m below the streambed. Figures 26 and 27 depict the results of the one-dimensional modeling efforts at the downstream transect for in-stream monitoring wells RW-044 and RW-035, respectively.

The streambed of the lower Merced River Basin proved to be a highly dynamic system, with mobile bar forms and substantial bed load transport during periods of low streamflow. High streamflow events also included suspended load. The model results in figures 26 and 27 depict periods where simulated temperatures nearly match observed temperatures. Periods of departure have three explanations: (1) they may be the result of the streambed characteristics changing over time, resulting in varying K values; (2) they may be a result of scour near wells that changes the effective depth of the temperature loggers and alters the model domain; and (3) the hydraulic head gradient that the model calculates is over a 2-m domain; however, changes in effective depth of pressure transducers that are due to scour near wells may not always coincide with the assumed model domain, resulting in calculated head gradients that are not representative of actual gradients.

Figure 26 depicts the simulated temperatures and modeled flux from March to September 2004 for monitoring well RW-044 and may be an exception to the explanations for departures from simulated temperatures as explained above. The pressure transducer in this monitoring well did not record a flow reversal during the April 2004 VAMP release and showed significant "noise" after the first data download in May 2004. The author of this report believes that this pressure transducer was faulty and failed after the second and last download in September 2004. The noise in the pressure-head data may explain why simulated temperatures were slightly higher than the actual temperatures recorded at approximately 0.5 and 1.0 m below the streambed.

Figure 27 depicts modeling results for monitoring well RW-035. Simulated temperatures match up until the dam release in October 2004. A departure from observed temperatures occurs during and following the dam release. The higher streamflow likely scoured out the fines accumulated over the summer prior to the October release, thereby increasing the streambed K. The departure of simulated temperatures from observed temperatures for this period indicates that for the simulated temperatures to continue to match the observed temperatures, the streambed K (and resultant vertical flux) must be higher than the model input value used prior to this period. Figure 28 depicts the results of a model run in which the streambed K was increased from 1 to 10 m/day for the period of departure (10/18/2004 to 1/25/2005). The resultant simulated temperatures for the departure period provide an improved match-to-observed temperatures and substantiate the interpretation for this departure. The resultant modeled vertical flux increased from 0.4 to 4.6 cm/day.

Although increasing hydraulic conductivity improves the simulated temperatures compared with the observed temperatures, it is difficult to accept that this factor alone explains the departure because it unlikely that vertical flux increased an order of magnitude over such a short period of time. Instead, a combination of factors may better explain the departure. It is likely that changes in effective depth of pressure transducers, attributed to scour near wells, resulted in instrumentation depth not coinciding with the assumed model domain. The result is that the head gradients that the model calculates are not representative of actual gradients. This explanation coupled with increased streambed K resulting from scouring of fines because of higher streamflow may provide a more accurate explanation of the departure.

Because of the data gap that occurs between January and February 2005 for monitoring well RW-035, and departure period following the October 2004 dam release, the model was run as three separate modeling periods. Table 9 lists the well name, modeling period, thermal conductivity, hydraulic conductivity, and average vertical flux input values of hydraulic, thermal conductivity, and average vertical flux.
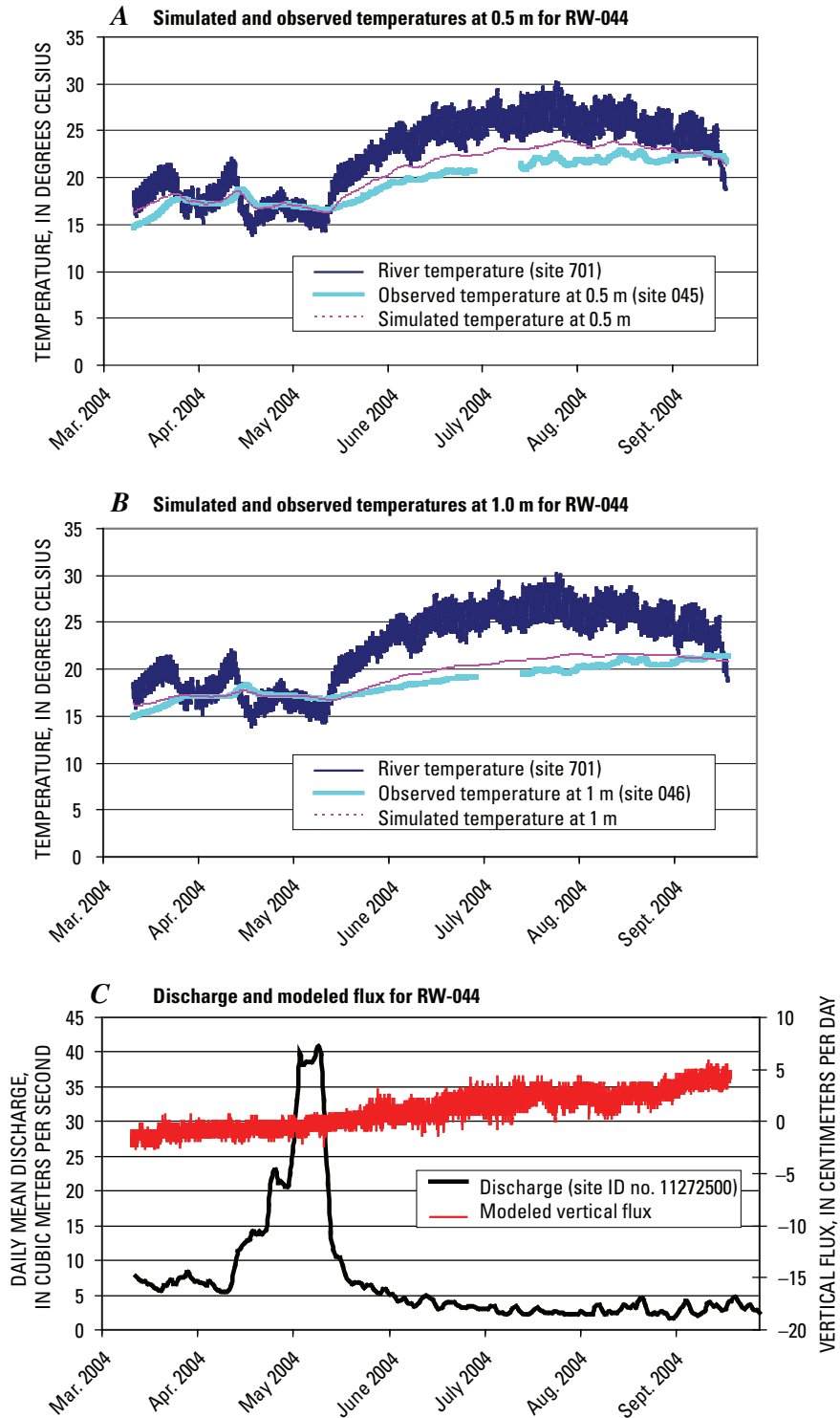
**Figure 26.**    Plots of observed and simulated temperatures for monitoring well RW-044. A. At 0.5 meters below the sediment–water interface. B. At 1 meter below the sediment–water interface. C. Resultant modeled vertical flux and stream discharge. The line breaks on the graphs represent missing data. The three digit site number in the Figure legend refers to the USGS site identification number with reference to figure 2 and table 1. (ID, identification; m, meter; no., number; RW, river well; USGS, U.S. Geological Survey.)
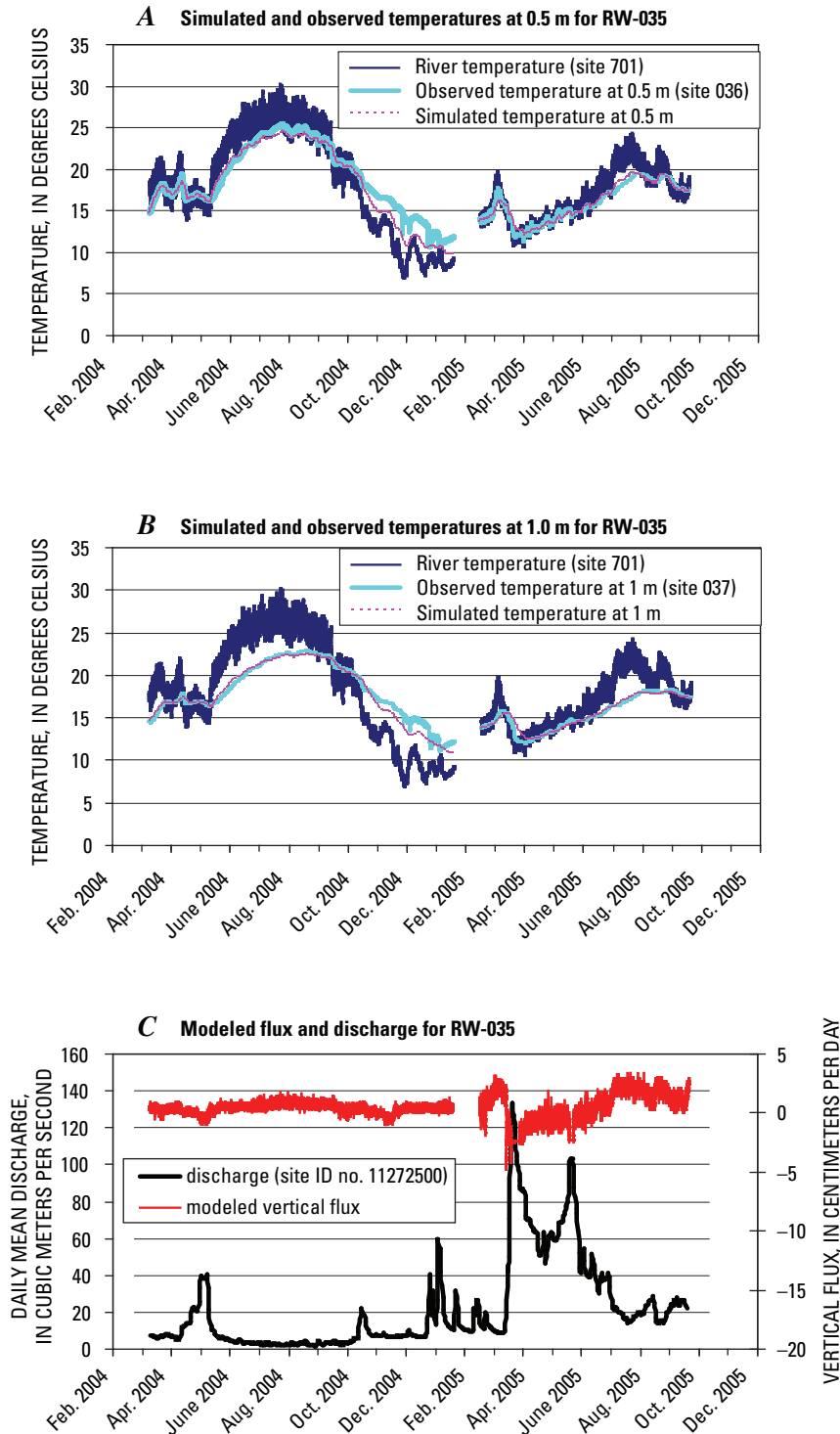
**Figure 27.**    Plots of observed and simulated temperatures for monitoring well RW-035. A. At 0.5 meters below the sediment–water interface. B. At 1 meter below the sediment–water interface. C. Modeled vertical flux and stream discharge. The line breaks on the graphs represent missing data. The three digit site number in the Figure legend refers to the USGS site identification number with reference to figure 2 and table 1. (ID, identification; m, meter; no., number; RW, river well; USGS, U.S. Geological Survey.)

**A**    Simulated and observed temperatures at 0.5 m for RW-035



**B**    Simulated and observed temperatures at 1.0 m for RW-035
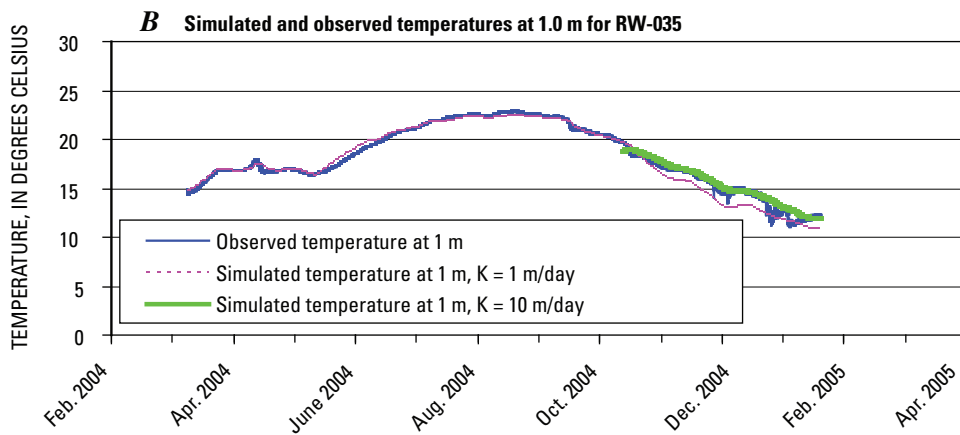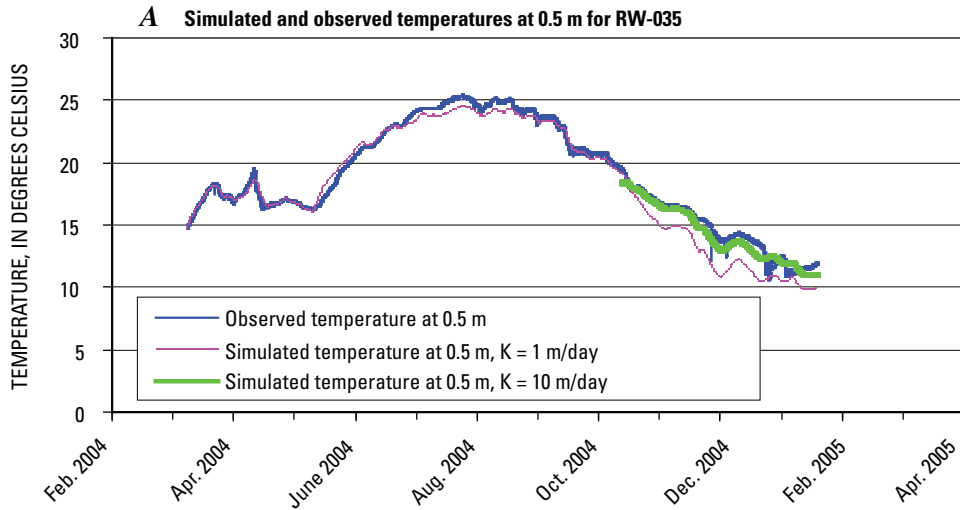


**Table 9.**    Modeling input values of listed parameters for modeling periods listed.

[°C, degrees Celsius; cm, centimeter; ID, identification; m, meter; RW, river well; W, watt]

| Monitoring well ID number | Modeling time period | Thermal conductivity (W/m °C) | Hydraulic conductivity (m/day) | Average vertical flux (cm/day) |
|---|---|---|---|---|
| RW-035 | 3/10/2004–10/18/2004 | 1.8 | 1.0 | 0.4 |
| RW-035 | [1]10/18/2004–1/25/2005 | 1.8 | 10 | 4.6 |
| RW-035 | 2/22/2005–10/2/2005 | 1.8 | 2.6 | 0.5 |
| RW-044 | 3/10/2004–9/20/2001 | 1.8 | 2.6 | 1.1 |

[1]Departure period depicted in figure 28.

# Conclusions

Estimates of vertical flux across the sediment–water interface were made by direct measurement using seepage meters and a heat as tracer method in a 100-m reach of the lower Merced River. Results of the temperature modeling efforts indicate that the Merced River at the study reach is generally a slightly gaining stream with very small head differences between surface water and ground water, and has flow reversals that can occur during high streamflow events. The period of study included a large range of streamflow that affected the streambed characteristics and hydraulic conductivity of the streambed. The high streamflow events associated with storm runoff events and large releases at the upstream dam resulted in an increase in hydraulic conductivity that probably was due to the scouring of fines accumulated during periods of low streamflow. The application of heat as a tracer method resulted in average vertical flux estimates across the sediment–water interface of 0.4–2.2 cm/day for the study period. The range of vertical hydraulic conductivities used in heat as a tracer model (VS2DH) was 1–10 m/day at the study reach.

The use of seepage meters to directly measure vertical flux generally failed in this high-energy system because of slow seepage rates and a mobile streambed that scoured or buried the seepage meters. Slug tests and grain-size analysis were directly compared to characterize the streambed hydraulic conductivity. Lateral hydraulic conductivities determined using slug tests ranged from 40 to 250 m/day at the upstream transect and from 10 to 100 m/day at the downstream transect. The locations of screened intervals likely explains variability in range of estimates. Variability in hydraulic conductivity for the grain-size method ranged from 50 to 110 m/day and 20 to 70 m/day for the upstream and downstream transects, respectively. The relative percent difference between hydraulic conductivity estimates by grain size and slug test for wells screened at 0.5 m below the sediment–water interface was 0–9 percent at the upstream transect and 80–133 percent at the downstream transect.

# References

Anderson, M.P., 2005, Heat as a ground water tracer: Ground Water, v. 46, no. 6, p. 951–968.

Asbury, C.E., 1990, The role of groundwater seepage in sediment chemistry and nutrient budgets in Mirror Lake, New Hampshire: Ithaca, N.Y., Cornell University, Ph.D. dissertation, 275 p.

Bartolino, J., and Niswonger, R., 1999, Temperature profiles of the aquifer system underlying the Rio Grande, N.M., Proceedings of Third Annual Middle Rio Grande Basin Workshop, Feb 22–23, 1999: U.S. Geological Survey Open-File Report 99-203, p. 66–67.

Bartow, J.A., 1991, The Cenozoic evolution of the San Joaquin Valley, California: U.S. Geological Survey Professional Paper 1501, 40 p.

Belanger, T.V., and Mikutel, D.F., 1985, On the use of seepage meters to estimate ground water nutrient loading to lakes: Water Resources Bulletin, v. 21, p. 265–271.

Belanger, T.V., and Montgomery, M.T., 1992, Seepage meter errors: Limnology and Oceanography, v. 37, no. 8, p. 1787–1795.

Blanchfield, P.J., and Ridgeway, M.S., 1996, Use of seepage meters to measure ground water flow at brook trout redds: Transactions of the American Fishery Society, v. 125, p. 813–818.

Bouwer, H., and Rice, R.C., 1976, A slug test method for determining hydraulic conductivity of unconfined aquifers with completely or partially penetrating wells: Water Resources Research, v. 12, no. 3, p. 423–428.

Boyle, D.R., 1994, Design of a seepage meter for measuring ground water fluxes in the nonlittoral zone of lakes—evaluation in a boreal forest lake: Limnology and Oceanography, v. 39, p. 670–681.

Brock, T.D., Lee, D.L., Janes, D., and Winek, D., 1982, Ground water seepage as a nutrient source to a drainage lake, Lake Mendota, Wisconsin: Water Research, v. 16, p. 1255–1263.

Brunke, M., and Gonser, T., 1997, The ecological significance of exchange processes between rivers and ground water: Freshwater Biology, v. 37, p. 1–33.

Burow, K.R., Shelton, J.L., Hevesi, J.A., and Weismann, G.S., 2004, Hydrogeologic characterization of the Modesto area, San Joaquin Valley, California: U.S. Geological Survey Scientific Investigations Report 2004-5232, 54 p.

Cable, J.E., Burnett, W.C., Chanton, J.P., Corbett, D.R., and Cable, P.H., 1997, Field evaluation of seepage meters in the coastal marine environment: Estuarine and Coastal Shelf Science, v. 45, p. 367–375.

Cey, E.E., Rudolph, D.L., Parkin, G.W., and Aravena, R., 1998, Quantifying ground water discharge to a small perennial stream in southern Ontario, Canada: Journal of Hydrology, v. 210, p. 21–37.

Chanton, J.P., Burnett, W.C., Dulaiova, H., Corbett, D.R., and Taniguchi, M., 2003, Seepage rate variability in Florida Bay drive by Atlantic tidal height: Biogeochemistry, v. 66, p. 187–202.

Cherkauer, D.A, and McBride, J.M., 1988, A remotely operated seepage meter for use in large lakes and rivers: Ground Water, v. 26, p. 165–171.

Choi, J., and Harvey, J.W., 2000, Quantifying time-varying ground-water discharge and recharge in wetlands of the northern Florida Everglades: Wetlands, v. 20, p. 500–511.

Connor, J.N., and Belanger, T.V., 1981, Ground water seepage in Lake Washington and the Upper St. Johns Basin, Florida: Water Resources Bulletin, v. 17, p. 799–805.

Constantz, J., 1998, Interaction between stream temperature, streamflow, and ground water exchanges in alpine streams: Water Resources Research, v. 34, no. 7, p. 1609–1615.

Constantz, J., Stewart, A.E., Niswonger, R., and Sarma, L., 2002, Analysis of temperature profiles for investigating stream losses beneath ephemeral channels: Water Resources Research, v. 38, no. 12, p. 52–1 to 52–13.

Constantz, J., Stonestrom, D., Stewart, A.E., Niswonger, R., and Smith, T.R., 2001, Analysis of streambed temperatures in ephemeral channels to determine streamflow frequency and duration: Water Resources Research, v. 37, no. 2, p. 317–328.

Constantz, J., and Thomas, C.L., 1997, Streambed temperature profiles as indicators of percolation characteristics beneath Arroyos in the Middle Rio Grande Basin, USA: Hydrological Processes, v. 11, p. 1621–1634.

Constantz, J., Thomas, C.L., and Zellweger, G., 1994, Influence of diurnal variations in stream temperature on streamflow loss and groundwater recharge: Water Resources Research, v. 30, no. 12, p. 3253–3264.

Croft, M.G., 1972, Subsurface geology of the late Tertiary and Quaternary water-bearing deposits of the southern part of the San Joaquin Valley, California: U.S. Geological Survey Water-Supply Paper 1999-H, 29 p.

Davies, W.J., 2002, Evaluation of diver water sensor and baro diver sensor: U.S. Geological Survey Water Resources Discipline Instrument News, issue 98, p. 11–18.

Davis, S.N., and Hall, F.R., 1959, Water-quality of the eastern Stanislaus and northern Merced counties, California: Stanford University Publications, Geological Sciences, v. 6, no. 1, 112 p.

Downing, J.A., and Perterka, J.J., 1978, The relationship of rainfall and lake ground water seepage: Limnology and Oceanography, v. 23, p. 821–825.

Dumouchelle, D.H., 2001, Evaluation of ground-water/surface-water relations, Chapman Creek, West-Central Ohio, by means of multiple methods: U.S. Geological Survey Water Resources Investigations Report 01-4202, 13 p.

Erickson, D.R., 1981, A study of littoral ground water seepage at Williams Lake, Minnesota, using seepage meters and wells: Minn., University of Minnesota, M.S. thesis, 153 p.

Fellows, C.R., and Brezonik, P.L., 1980, Seepage flow into Florida lakes: Water Resources Bulletin, v. 16, p. 635–641.

Fetter, C.W., 2001, Applied Hydrogeology: New York, N.Y., Macmillan College Publishing Company, 598 p.

Findlay, S., 1995, Importance of surface–subsurface exchange in stream ecosystems—the hyporheic zone: Limnology and Oceanography, v. 40, no. 1, p. 159–164.

Fryar, A.E., Wallin, E.J., and Brown, D.L., 2000, Spatial and temporal variability in seepage between a contaminated aquifer and tributaries to the Ohio River: Ground Water Monitoring Remediation, v. 20, p. 129–146.

Gilbert, J., Danielopol, D.L., and Stanford, J.A., 1994, Ground Water Ecology: San Diego, Calif., Academic Press, 571 p.

Gronberg, J.M, and Kratzer, C.R., 2006, Environmental setting of the lower Merced River basin, California: U.S. Geological Survey Scientific Investigations Report 2006-5152, 37 p.

Harvey, F.E., and Lee, D.R., 2000, Discussion of "The effects of bag type and meter size on seepage meter measurements": Ground Water, v. 38, p. 326–328.

Harvey, J.W., and Wagner, B.J., 2000, Quantifying hydrologic interactions between steams and their subsurface hyporheic zones *in* Streams and Ground Waters: New York, N.Y., Academic Press, p. 3–44.

Hazen, A., 1911, Discussion—dams of sand foundations: Transactions, American Society of Civil Engineers, v. 73, 1999.

Healy, R.W., and Ronan, A.D., 1996, Documentation of computer program VS2DH for simulation of energy transport in variably saturated porous media—modification of the U.S. Geological Survey's computer program VS2DT: U.S. Geological Survey Water-Resources Investigations Report 96-4230, 36p. [Also available at http://pubs.er.usgs.gov/pubs/wri/wri964230]

Hsieh, P.A., Wingle, W., and Healy, R.W., 2000, VS2DI—a graphical software package for simulating fluid flow and solute or energy transport in variably saturated porous media: U.S. Geological Survey Water-Resources Investigations Report 99-4130, 16 p.

Isiorho, S.A., and Matisoff, G., 1990, Ground water recharge from Lake Chad: Limnology and Oceanography, v. 35, p. 931–938.

Isiorho, S.A., and Meyer, J.H., 1999, The effects of bag type and meter size on seepage meter measurements: Ground Water, v. 37, no. 3, p. 411–413.

Israelsen, O.W., and Reeve, R.C., 1944, Canal lining experiments in the Delta Area: Utah Technical Bulletin 313, Utah Agricultural Experiment Station, Logan, Utah.

Jackman, A.P., Triska, F.J., and Duff, J.H., 1997, Hydrologic examination of ground water discharge into the upper Shingobee River: U.S. Geological Survey Water Resources Investigations Report 96-4215, p. 137–147.

John, P.H., and Lock, M.A., 1977, The spatial distribution of ground water discharge into the littoral zone of a New Zealand Lake: Journal of Hydrology, v. 33, p. 391–395.

Kelly, S.E., 2001, Methods for determining the hydrologic characteristics of streambeds: Clemson, S.C., Clemson University, M.S. thesis, 111 p.

Kratzer, C.R., and Biagtan, R.N., 1997, Determination of traveltimes in the lower San Joaquin River Basin, California, from dye-tracer studies during 1994–1995: U.S. Geological Survey Water-Resources Investigations Report 97-4018, 20 p.

Landon, M.K., Rus, D.L., and Harvey, F.E., 2001, Comparison of in-stream methods of measuring hydraulic conductivity in sandy streambeds: Ground Water, v. 39, p. 870–885.

Lapham, W.W., 1988, Conductive and convective heat transfer in sediments near streams: Tucson, Ariz., University of Arizona, Ph.D. dissertation, 315 p.

Lapham, W.W., 1989, Use of temperature profiles beneath streams to determine rates of vertical ground-water flow and vertical hydraulic conductivity: U.S. Geological Survey Water-Supply Paper 2337, 35 p.

Lee, D.R., 1977, A device for measuring seepage flux in lakes and estuaries: Limnology and Oceanography, v. 22, p. 140–147.

Lee, D.R., and Cherry, J.A., 1978, A field exercise on ground water flow using seepage meters and mini-piezometers: Journal of Geology Education, v. 27, p. 6–10.

Lee, D.R., and Hynes, H.B., 1977, Identification of ground water discharge zones in a reach of Hillman Creek in Southern Ontario: Water Pollution Resources Canada, v. 13, p. 121–133.

Lesack, L.F., 1995, Seepage exchange in an Amazon floodplain lake: Limnology and Oceanography, v. 40, p. 598–609.

Libelo, L.E., and MacIntyre, W.G., 1994, Effects of surface-water movement on seepage meter measurements of flow through the sediment–water interface: Applied Hydrogeology, v. 4, p. 49–54.

Linderfelt, W.R., and Turner, J.V., 2001, Interaction between shallow ground water, saline surface water and nutrient discharge in a seasonal estuary—the Swan-Canning system: Hydrological Processes, v. 15, p. 2631–2653.

Lock, M.A., and John, P.A., 1978, The measurement of ground water discharge into a lake by a direct method: International Review of Hydrobiology, v. 63, p. 271–275.

McBride, J.M., 1987, Measurement of ground water flow to the Detroit River, Michigan and Ontario: Milwaukee, Wis., University of Wisconsin–Milwaukee, MS thesis.

Modesto Irrigation District, 2005, Precipitation and temperature data for 1988–2005 for Modesto. Accessed Nov. 15, 2006, at http://www.mid.org/wthr-hist.htm

Murdoch, L.C., and Kelly, S.E., 2003, Factors affecting the performance of conventional seepage meters: Water Resources Research, v. 39, no. 6, p. 2-1 to 2-10.

Page, R.W., 1977, Appraisal of ground-water conditions in Merced, California, and vicinity: U.S. Geological Survey Open-File Report 77-454, 43 p.

Page, R.W., 1986, Geology of the fresh ground-water basin of the Central Valley, California, with texture maps and sections: U.S. Geological Survey Professional Paper 1401-C, 54 p., 5 pls.

Page, R.W., and Balding, G.N., 1973, Geology and quality of water in the Modesto–Merced area, San Joaquin Valley, California: U.S. Geological Survey Water Resources Investigations Report 73-6, 85 p.

Paulsen, R.J., Smith, C.F., O'Rourke, D., and Wong, T.F., 2001, Development and evaluation of an ultrasonic ground water seepage meter: Ground Water, v. 39, p. 904–911.

Penman, H.L., 1963, Vegetation and hydrology: Farnham Royal, England, Commonwealth Bureau of Soil Technology, Communication, v. 53, 124 p.

Rorabaugh, M.I., 1954, Streambed percolation in development of water supplies: U.S. Geological Survey Ground Water Notes on Hydraulics, no. 25, 13 p.

Rosenberry, D.O., 2000, Unsaturated-zone wedge beneath a large, natural lake: Water Resources Research, v. 36, p. 3401–3409.

Rosenberry, D.O, 2005, Integrating seepage heterogeneity with the use of ganged seepage meters: Limnology and Oceanography: Methods, v. 3, p. 131–142.

Rosenberry, D.O., and Morin, R.J., 2004, Use of an electromagnetic seepage meter to investigate temporal variability in lake seepage: Ground Water, v. 41, p. 68–77.

Schincariol, R.A., and McNeil, J.D., 2002, Errors with small volume elastic seepage bags: Ground Water, v. 40, p. 649–651.

Sebestyen, S.D., and Schneider, R.L., 2001, Dynamic temporal patterns of nearshore seepage flux in a headwater Adirondack Lake: Journal of Hydrology, v. 247, p. 137–150.

Shaw, R.D., and Prepas, E.E., 1989, Anomalous, short-term influx of water into seepage meters: Limnology and Oceanography, v. 34, no. 7, p. 1343–1351.

Shaw, R.D., and Prepas, E.E., 1990a, Ground water–lake interactions—I. Accuracy of seepage meter estimates of lake seepage: Journal of Hydrology, v. 119, p. 105–120.

Shaw, R.D., and Prepas, E.E., 1990b, Ground water–lake interactions—II. Nearshore seepage patterns and the contribution of ground water to lakes in central Alberta: Journal of Hydrology, v. 112, p. 121–136.

Shaw, R.D., Shaw, J.F.H., Fricker, H., and Prepas, E.E., 1990, An integrated approached to quantify ground water transport of phosphorus to Narrow Lake, Alberta: Limnology and Oceanography, v. 35, p. 870–886.

Shinn, E.A., Reich, C.D., and Hickey, T.D., 2002, Seepage meters and Bernoulli's revenge: Estuaries, v. 25, p. 126–132.

Silliman, S.E., and Booth, D.F., 1993, Analysis of time-series measurements of sediment temperature for identification of gaining vs. losing portions of Juday Creek, Indiana: Journal of Hydrology, v. 146, p. 131–148.

Silliman, S.E., Ramirez, J., and McCabe, R.L., 1995, Quantifying downflow through creek sediments using temperature time series—one-dimensional solution incorporating measured surface temperature: Journal of Hydrology, v. 167, p. 99–119.

Sorey, M.L., 1971, Measurement of vertical ground water velocity from temperature profiles in a well: Water Resources Research, v. 7, p. 963–970.

Stallman, R.W., 1963, Methods of collecting and interpreting ground-water data: U.S. Geological Survey Water-Supply Paper 1544-H, p. 36–46.

Stillwater Sciences and EDAW Inc., 2001, Merced River corridor restoration plan baseline studies, vol. I—identification of social, institutional and infrastructural opportunities and constraints, Final Report, 54 p. Accessed May 7, 2006, at http://www.stillwatersci.com/publications/reports/

Stonestrom, D.A., and Constantz, J., eds., 2003, Heat as a tool for studying the movement of ground water near streams: U.S. Geological Survey Circular 1260, 96 p.

Stonestrom, D.A., and Constantz, J., 2004, Using temperature to study stream–ground water exchanges: U.S. Geological Survey Fact Sheet 2004-3010.

Suzuki, S., 1960, Percolation measurements based on heat flow through soil with special reference to paddy fields: Journal of Geophysical Research, v. 65, p. 2883–2885.

Taniguchi, M., 2002, Tidal effects on submarine groundwater discharge into the ocean: Geophysical Research Letters, p. 29.

Taniguchi, M., and Fukuo, Y., 1993, Continuous measurements of ground water seepage using an automatic seepage meter: Ground Water, v. 31, no. 7, p. 675–679.

Taylor, C.A., and Nickle, H.G., 1936, Investigations in Cold Canyon: California Division of Water Resources Bulletin 37, p. 88–121.

Troxell, H.C., 1936a, Ground water supply and natural losses in the valley of Santa Ana River between Riverside Narrows and the Orange county line: California Department of Water Resources Bulletin 37, p. 147–172.

Troxell, H.C., 1936b, The diurnal fluctuation in the groundwater and flow of the Santa Ana River and its meaning: Eos Transactions, American Geophysical Union, v. 17, p. 498–507.

Vogelmann, J.E., Howard, S.M., Yang, L., Larson, C.R., Wylie, B.K., and Van Driel, Nick, 2001, Completion of the 1990s national land cover dataset for the conterminous United States from Landsat Thematic Mapper data and ancillary data sources: Photogrammetric Engineering and Remote Sensing, v. 67, p. 650–652.

Winter, T.C., Harvey, J.W., Franke, O.L., and Alley, W.M., 1998, Ground water and surface water—a single resource: U.S. Geological Survey Circular 1139, 79 p.

Wisler, C.O., and Brater, E.F., 1959, Hydrology: New York, N.Y., John Wiley, 408 p.

Woessner, W.W., and Sullivan, K.E., 1984, Results of seepage meter and mini-piezometer study, Lake Mead, Nevada: Ground Water, v. 22, p. 561–568.

Wrobicky, G.L., Campana, M.E., Vallet, H.M., and Dahm, C.N., 1998, Seasonal variation in surface–subsurface water exchange and lateral hyporheic area of two stream–aquifer systems: Water Resources Research, v. 34, no. 3, p. 317–332.

Yelverton, G.F., and Hackney, C.T., 1986, Flux of dissolved organic carbon and pore water through the substrate of a *Spartina alterflora* marsh in North Carolina: Estuarine and Coastal Shelf Science, v. 22, p. 255–267.

Zimmerman, C.F., Montgomery, J.R., and Carlson, P.R., 1985, Variability of dissolved reactive phosphate flux rates in nearshore estuarine sediments—effects of ground water flow: Estuaries, v. 8, p. 228–236.

## Appendix

[cm, centimeter; ID, identification; mL, milliliter; PC, parameter code]

Sampling Event 1

December 2–4, 2003

| USGS site ID number | Seepage meter | Bag type | Hyporheic flux of water from ground water to surface water (mL/cm²/day) PC 99066 | Hyporheic flux of water from ground water to surface water (mL/cm²/day) PC 99066 |
|---|---|---|---|---|
| | | | December 2–3, 2003 | December 3–4, 2003 |
| 372312120480007 | A | shower bag | 0.01 | –0.5 |
| 372312120480008 | 1 | medical bag | –1.5 | –1.1 |
| 372312120480009 | B | shower bag | –0.16 | 0.11 |
| 372312120480010 | 2 | medical bag | –2.1 | –2.2 |
| 372312120480011 | C | shower bag | 0.24 | 0.2 |
| 372312120480012 | 3 | medical bag | lost stopper | 0.5 |
| 372312120480001 | D | shower bag | 0.02 | 0.16 |
| 372312120480002 | 4 | medical bag | –1.5 | –1.7 |
| 372312120480003 | E | shower bag | 0.07 | 0.15 |
| 372312120480004 | 5 | medical bag | 0.06 | 1.2 |
| 372312120480005 | F | shower bag | –0.48 | –0.08 |
| 372312120480006 | 6 | medical bag | 0.19 | –0.48 |

Sampling Event 2

January 29–31, 2004

| USGS site ID number | Seepage meter | Bag type | Hyporheic flux of water from ground water to surface water (mL/cm²/day) PC 99066 | Hyporheic flux of water from ground water to surface water (mL/cm²/day) PC 99066 |
|---|---|---|---|---|
| | | | January 29–30, 2004 | January 30–31, 2004 |
| 372312120480007 | A | shower bag | 0.05 | 0.06 |
| 372312120480008 | 1 | medical bag | 0.19 | 0.89 |
| 372312120480009 | B | shower bag | 0.2 | 0.24 |
| 372312120480010 | 2 | medical bag | –0.57 | 0.13 |
| 372312120480011 | C | shower bag | 0.15 | 0.15 |
| 372312120480012 | 3 | medical bag | –1.2 | –1.9 |
| 372312120480001 | D | shower bag[1] | 0.15 | –0.01 |
| 372312120480002 | 4 | medical bag[1] | –0.03 | –1.9 |
| 372312120480003 | E | shower bag[1] | 0.13 | complete scour of meter |
| 372312120480004 | 5 | medical bag[1] | –1.7 | –2.2 |
| 372312120480005 | F | shower bag[1] | 0.18 | –0.43 |
| 372312120480006 | 6 | medical bag[1] | –0.22 | –1.9 |

[1]Indicates shower bag used in the first 24-hour measurement period and packaging bag used in the second 24-hour measurement period.

**Appendix**–Continued.

[cm,centimeter; ID, identification; mL, milliliter; PC, parameter code]

| | | | Sampling Event 3 | |
|---|---|---|---|---|
| | | | February 10–12, 2004 | |
| **USGS site ID number** | **Seepage meter** | **Bag type** | **Hyporheic flux of water from ground water to surface water (mL/cm²/day) PC 99066** | **Hyporheic flux of water from ground water to surface water (mL/cm²/day) PC 99066** |
| | | | February 10–11, 2004 | February 11–12, 2004 |
| 372312120480007 | A | shower  bag | 0.2 | 0.17 |
| 372312120480008 | 1 | medical bag | 0.83 | 0.16 |
| | | | | |
| 372312120480009 | B | shower  bag | 0.07 | –0.02 |
| 372312120480010 | 2 | medical bag | –2.1 | –2 |
| | | | | |
| 372312120480011 | C | shower  bag | 0.18 | 0.01 |
| 372312120480012 | 3 | medical bag | 0.03 | –0.79 |
| | | | | |
| 372312120480001 | D | shower  bag[1] | –0.03 | –0.02 |
| 372312120480002 | 4 | medical bag[1] | –1.4 | –2 |
| | | | | |
| 372312120480003 | E | shower  bag[1] | 0.13 | 0.11 |
| 372312120480004 | 5 | medical bag[1] | –2 | 1.3 |
| | | | | |
| 372312120480005 | F | shower  bag[1] | –0.04 | 0.56 |
| 372312120480006 | 6 | medical bag[1] | –0.06 | 0.2 |

[1]Indicates shower bag used in the first 24-hour measurement period and packaging bag used in the second 24-hour measurement period.

| | | | Sampling Event 4 | |
|---|---|---|---|---|
| | | | July 19–21, 2004 | |
| **USGS site ID number** | **Seepage meter** | **Bag type** | **Hyporheic flux of water from ground water to surface water (mL/cm²/day) PC 99066** | **Hyporheic flux of water from ground water to surface water (mL/cm²/day) PC 99066** |
| | | | July 19–20, 2004 | July 20–21, 2004 |
| 372312120480007 | A | packaging bag | 0.43 | 0.61 |
| 372312120480008 | 1 | packaging bag | –1.3 | 0.45 |
| | | | | |
| 372312120480009 | B | packaging bag | 0.46 | –0.1 |
| 372312120480010 | 2 | packaging bag | –1.6 | 4.3 |
| | | | | |
| 372312120480011 | C | packaging bag | 0.38 | 0.71 |
| 372312120480012 | 3 | packaging bag | 2.8 | 4.2 |
| | | | | |
| 372312120480001 | D | packaging bag | 0.39 | –0.23 |
| 372312120480002 | 4 | packaging bag | –1.7 | 1.2 |
| | | | | |
| 372312120480003 | E | packaging bag | 0.11 | 0.75 |
| 372312120480004 | 5 | packaging bag | housing unit dislodged | 4.2 |
| | | | | |
| 372312120480005 | F | packaging bag | 0.35 | 0.58 |
| 372312120480006 | 6 | packaging bag | 0.79 | –0.41 |

**Appendix**–Continued.

[cm,centimeter; ID, identification; mL, milliliter; PC, parameter code]

| | | | Sampling Event 5 | |
| | | | September 20–22, 2004 | |
| USGS site ID number | Seepage meter | Bag type | Hyporheic flux of water from ground water to surface water (mL/cm²/day) PC 99066 | Hyporheic flux of water from ground water to surface water (mL/cm²/day) PC 99066 |
| --- | --- | --- | --- | --- |
| | | | September 20–21, 2004 | September 21–22, 2004 |
| 372312120480007 | A | packaging bag | 0.31 | 0.23 |
| 372312120480008 | 1 | packaging bag | –0.16 | –0.11 |
| 372312120480009 | B | packaging bag | collection bag disconnected | 0.43 |
| 372312120480010 | 2 | packaging bag | –1.1 | –0.63 |
| 372312120480011 | C | packaging bag | –0.05 | 0.52 |
| 372312120480012 | 3 | packaging bag | –1.1 | –0.23 |
| 372312120480001 | D | packaging bag | hole developed in collection bag | 0.4 |
| 372312120480002 | 4 | packaging bag | 0.14 | 0.77 |
| 372312120480003 | E | packaging bag | 0.6 | –0.11 |
| 372312120480004 | 5 | packaging bag | –1 | –0.55 |
| 372312120480005 | F | packaging bag | 0.43 | 0.03 |
| 372312120480006 | 6 | packaging bag | –0.9 | 0.12 |

| | | | Sampling Event 6 | |
| | | | September 22–23, 2004 | |
| USGS site ID number | Seepage meter | Bag type | Hyporheic flux of water from ground water to surface water (mL/cm²/day) PC 99066 | Hyporheic flux of water from ground water to surface water (mL/cm²/day) PC 99066 |
| --- | --- | --- | --- | --- |
| | | | September 21–22, 2004 | September 22–23, 2004 |
| 372312120480007 | A | packaging bag | 0.23 | 0.14 |
| 372312120480008 | 1 | packaging bag | –0.11 | 0.46 |
| 372312120480009 | B | packaging bag | 0.43 | 0.11 |
| 372312120480010 | 2 | packaging bag | –0.63 | 1 |
| 372312120480011 | C | packaging bag | 0.52 | 0.06 |
| 372312120480012 | 3 | packaging bag | –0.23 | –1.2 |
| 372312120480001 | D | packaging bag | 0.4 | 0.12 |
| 372312120480002 | 4 | packaging bag | 0.77 | 0.8 |
| 372312120480003 | E | packaging bag | –0.11 | 0.27 |
| 372312120480004 | 5 | packaging bag | –0.55 | 1.3 |
| 372312120480005 | F | packaging bag | 0.03 | –0.15 |
| 372312120480006 | 6 | packaging bag | 0.12 | –0.4 |

This page intentionally left blank.

USGS